mmol) was dissolved in 2 mL of CH_2Cl_2, cooled to −78 °C, and $HBF_4 \cdot Et_2O$ (0.05 mL, 0.06 g, 0.37 mmol) was added slowly with stirring. Ether was added to complete the precipitation of the product. The yellow solid was filtered, washed with ether, and recrystallized from acetone/ether at 0 °C to give (*S*)-**21**, 90.0 mg (81%).

Preparation of (*S*)-Lactone 20. The salt above was taken up in 4 mL of nitromethane, cooled to 0 °C, and treated with 10% molar excess of NEt_3. The solvent was removed in vacuo, leaving an orange yellow oil, which was chromatographed on basic alumina (III) with ether/CH_2Cl_2

to give the (*S*)-lactone **20** (70.0 mg 75%): $[\alpha]^{25}_D = -292°$ (*c* 0.1, CH_3CN).

Molecular Metals with Widely Tunable Band Filling. Structure/Stoichiometry/Counterion Relationships in the Electrochemistry of a Cofacially Joined Polymeric Phthalocyanine Metal

John G. Gaudiello, Glen E. Kellogg, Stephen M. Tetrick, and Tobin J. Marks*

Contribution from the Department of Chemistry and the Materials Research Center, Northwestern University, Evanston, Illinois 60208. Received July 18, 1988

Abstract: The oxidative electrochemistry of the cofacially joined phthalocyanine polymer $[Si(Pc)O]_n$ to yield molecular metals/conductive polymers of the type $\{[Si(Pc)O]X_y\}_n$ is studied by a combination of X-ray diffractometric and spectroscopic techniques. Electrochemical methodology includes controlled-potential coulometry and electrochemical potential spectroscopy (ECPS) applied to rapidly stirred slurries or to microcompactions of the solid polymer. For $X^- = BF_4^-$ in acetonitrile, oxidation ("doping") of as-polymerized orthorhombic $[Si(Pc)O]_n$ to yield tetragonal $\{[Si(Pc)O](BF_4)_y\}_n$ ($y \approx 0.50$) is accompanied by a significant overpotential, minimal tunability in y, and involves a first-order structural phase transformation. Electrochemical undoping occurs smoothly and over a broader potential range (0.90 V) to afford tetragonal $[Si(Pc)O]_n$, which is also accessible by thermally undoping $\{[Si(Pc)O]I_{1.1}\}_n$. Once in the more open tetragonal structure, both the electrochemical and diffraction data argue that y (hence, conduction band filling) can be homogeneously/continuously tuned between 0.0 and 0.50. This result verifies the crystal structural basis of the polymer electrochemical "break-in" phenomenon. It also represents the first case in which the band filling of a molecular metal is broadly tunable. In tetrahydrofuran, tetragonal $[Si(Pc)O]_n$ can also be reversibly *n*-doped to yield $\{[N(n\text{-butyl})_4]_{0.09}[Si(Pc)O]\}_n$. Oxidative ECPS studies with a number of anions in acetonitrile (PF_6^-, SbF_6^-, tosylate, $CF_3(CF_2)_nSO_3^-$, $n = 0, 3, 7$) demonstrate that maximum doping stoichiometries achievable (y, hence band filling) are largely a function of anion size, i.e., packing constraints within the tetragonal $\{[Si(Pc)O]X_y\}_n$ crystal structure. In contrast to these results, ECPS studies of solid $Ni(Pc)$ (monoclinic slipped-stack β phase) reveal a first-order structural transformation to yield tetragonal $Ni(Pc)(BF_4)_y$ ($y \approx 0.48$) upon oxidative doping, and a subsequent first-order transformation to another slipped-stack $Ni(Pc)$ structure (monoclinic slipped-stack γ phase) upon undoping. Doping/undoping occurs over a relatively narrow potential range; consequently there is far less tunability in y than in the $\{[Si(Pc)O]X_y\}_n$ materials, and large overpotentials are observed. ECPS studies of $[Ge(Pc)O]_n$ reveal irreversible oxidative processes, and polymer decomposition via Ge–O bond cleavage is implicated.

The electrical, optical, and magnetic properties of "molecular metals"[1] are a delicate function of complex architectural and electronic structural interactions that, traditionally, have been both difficult to control and to disentangle. For example, attempts to introduce potentially informative electronic structural perturbations have typically been frustrated by concurrent and unavoidable changes in crystal structure. Over the past several years, we have demonstrated that robust, highly crystalline, and structurally well-defined macromolecules of the type $[M(Pc)O]_n$ (A: M =
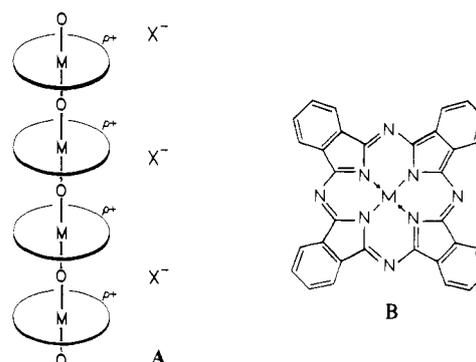
Si, Ge, Sn; Pc = phthalocyaninato, B)[2] offer an unprecedented opportunity to sequentially vary many of the essential charac-

(1) (a) *Proc. Int. Conf. Sci. Technol. Synth. Met., Synth. Met.* **1987**, *17–19*. (b) Ferraro, J. R.; Williams, J. M. *Introduction to Synthetic Electrical Conductors*; Academic Press: New York, 1987. (c) Jĕrome, D., Caron, L. G., Eds. *Low-Dimensional Conductors and Superconductors*; Plenum: New York, 1987. (d) Becker, J. Y., Bernstein, J., Bittner, S., Eds. *Isr. J. Chem.* **1986**, *27*(4). (e) Cowan, D. O.; Wiygul, F. M. *Chem. Eng. News* **1986**, *64*(29), 28–45. (f) Cohen, M. L. *Science* **1986**, *234*, 549–553. (g) Williams, J. M. *Prog. Inorg. Chem.* **1985**, *33*, 183–220. (h) Wudl, F. *Acc. Chem. Res.* **1984**, *17*, 227–232. (i) Greene, R. L.; Street, G. B. *Science* **1984**, *226*, 651–656. (j) Miller, J. S., Ed. *Extended Linear Chain Compounds*; Plenum: New York, 1982; Vol. 1–3.

(2) (a) Marks, T. J. *Science* **1985**, *227*, 881–889. (b) Marks, T. J.; Kalina, D. W. In ref 1j, Vol. 1, pp 197–331.

teristics of a metallophthalocyanine molecular metal[3] while rigorously enforcing the stacking architecture of the charge-transporting $Pc^{\rho+}$ radical-cation arrays.[4] In recent work, we explored the effects on $[M(Pc^{\rho+})O]_n$ collective properties of sequentially varying the Pc–Pc interplanar stacking separation (hence, bandwidth)[5,6] and the chemically introduced, charge-compensating off-axis counterions (X^- in A).[7] For oxidants such as halogens and nitrosonium salts, the latter studies revealed inhomogeneous "doping" (oxidation), an essentially invariant degree of partial oxidation [$\rho \approx +0.35$ (3)],[7] and a marked insensitivity of optical, magnetic, and electrical properties to the identity of a rather narrow range of X^-. Such results immediately raise the fascinating question of how this structure-enforced molecular metal might respond to far more drastic architectural and electronic structural perturbations. This is the subject of the present contribution.

We report here a full discussion of our studies of $[M(Pc)O]_n$ electrochemistry.[8] It is seen that the first wide tunability in the band filling of a molecular metal can be achieved [in contrast to the *fixed* values traditionally obtained, e.g., $TTF^{+0.59}TCNQ^{-0.59}$, $(TMTSF^{+0.5})_2X^-$, $(BEDT-TTF^{+0.5})_2X^-$, etc.][1,9] and that this molecular metal can be both p- and n-doped. Furthermore, the structurally well-defined character of the present starting materials and products affords valuable information on conductive polymer[10]

electrochemistry[10,11] (current/voltage characteristics, limiting doping level as a function of X^-, etc.) which has implications for many other conductive polymers. Finally, we report an electrochemical slurry doping technique which may have general applicability, and probe the role of the $(-SiO-)_n$ backbone by comparative solid-state electrochemical studies of Ni(Pc).

It is also of great interest to understand how the diverse collective properties of a molecular metal vary as a function of broad excursions in band filling and X^-. This complementary study of the aforementioned electrochemically prepared $\{[Si(Pc)O]X_y\}_n$ materials is the subject of the accompanying contribution.[12]

Experimental Section

Materials. Solvents used for synthesis were purified as follows: quinoline was vacuum distilled from BaO; pyridine was distilled under N_2 from BaO, benzene and chloroform from P_2O_5 (twice each) under high vacuum, and methanol from Mg under N_2. The reagent $SiCl_4$ was distilled under N_2; Ni(Pc) (Kodak) was vacuum sublimed twice [400 °C (10^{-4} Torr)]. Elemental analyses for synthesized electrolytic salts and for doped molecular metal materials were performed by Galbraith Laboratories. The acetonitrile used for electrochemical measurements was obtained from MCB (Omnisolv grade) and was purified and dried by either the literature procedure[13] or by distillation three times under high vacuum from P_2O_5. Electrochemical redox properties of the acetonitrile prepared by either method were identical by cyclic voltammetry (CV). Tetrahydrofuran (THF) was dried by storage over sodium and then vacuum transferred onto Na/K alloy. After being stirred for 24 h, the THF was vacuum transferred into a flame-dried storage flask containing Na/K alloy, freeze–pump–thaw degassed, and stored attached to the high-vacuum line. The supporting electrolytes used for these studies were obtained from the following sources: tetra-*n*-butylammonium tetrafluoroborate [$(n\text{-}Bu_4N^+)BF_4^-$], tetraethylammonium *p*-toluenesulfonate [$(Et_4N^+)TOS^-$], and tetra-*n*-butylammonium hexafluorophosphate [$(n\text{-}Bu_4N^+)PF_6^-$] from Southwestern Analytical Chemical; tetra-*n*-butylammonium trifluoromethanesulfonate [$(n\text{-}Bu_4N^+)CF_3SO_3^-$] and tetraethylammonium perfluoro-*n*-octanesulfonate [$(Et_4N^+)PFOS^-$] from Fluka Chemical; and tetra-*n*-butylammonium hexafluoroantimonate [$(n\text{-}Bu_4N^+)SbF_6^-$], tetra-*n*-butylammonium nonafluoro-*n*-butanesulfonate [$(n\text{-}Bu_4N^+)NFBS^-$], tetra-*n*-butylammonium 1-pyrenesulfonate [$(n\text{-}Bu_4N^+)PYS^-$], and tetra-*n*-butylammonium sulfate [$(n\text{-}Bu_4N^+)_2SO_4^{2-}$] were prepared as described below. The electrochemical windows and purity of these electrolyte salts were checked in dry acetonitrile by using cyclic voltammetry. Where necessary the salts were recrystallized from acetone/ether, washed with ether, and vacuum dried. This procedure (CV/recrystallization) was repeated until the electrolyte salt showed no significant redox processes in the -1.5 to $+2.5$ V usable electrochemical window of acetonitrile.

Synthesis of Orthorhombic $[Si(Pc)O]_n$. $Si(Pc)Cl_2$ was prepared as described previously,[5a] with the following modifications. The reagent 1,3-diiminoisoindoline was recrystallized from hot MeOH immediately before use. The crude $Si(Pc)Cl_2$ was washed with dry chloroform on filter paper rather than on a frit to avoid contamination from glass microparticles. This product was additionally washed by Soxhlet extraction with MeOH for 16 h under N_2 to remove unreacted 1,3-diiminoisoindoline. The room temperature magnetic susceptibility of Si(Pc)Cl₂ prepared and purified in this manner is in agreement with the value reported earlier ($\chi = -4.908 \times 10^{-4}$ emu/mol).[5b,7a] Sublimation of $Si(Pc)Cl_2$ [420 °C (10^{-4} Torr)] causes a significant amount of decomposition and occasionally yields a material with an unidentified paramagnetic impurity. The dihydroxide monomer $Si(Pc)(OH)_2$ and the polymer $[Si(Pc)O]_n$ ($n \geq 100$)[5a] were synthesized from the dichloride as previously described.[5a]

(3) (a) Almeida, M.; Kanatzidis, M. G.; Tonge, L. M.; Marks, T. J.; Marcy, H. O.; McCarthy, W. J.; Kannewurf, C. R. *Solid State Commun.* **1987**, *65*, 457–461. (b) Inabe, T.; Liang, W.-B.; Lomax, J. F.; Nakamura, S.; Lyding, J. W.; McCarthy, W. J.; Carr, S. H.; Kannewurf, C. R.; Marks, T. J. *Synth. Met.* **1986**, *13*, 219–229. (c) Inabe, T.; Nakamura, S.; Liang, W.-B.; Marks, T. J.; Burton, R. L.; Kannewurf, C. R.; Imaeda, K.-I. *J. Am. Chem. Soc.* **1985**, *107*, 7224–7226. (d) Inabe, T.; Marks, T. J.; Burton, R. L.; Lyding, J. W.; McCarthy, W. J.; Kannewurf, C. R.; Reisner, G. M.; Herbstein, F. H. *Solid State Commun.* **1985**, *54*, 501–503. (e) Martinsen, J.; Palmer, S. M.; Tanaka, J.; Greene, R. C.; Hoffman, B. M. *Phys. Rev. B* **1984**, *30*, 6269–6276. (f) Yakushi, K.; Sakuda, M.; Hamada, I.; Kuroda, H.; Kawamoto, A.; Tanaka, J.; Sugano, T.; Kinoshita, M. In ref 1a, *19*, 769–775. (g) Schramm, C. J.; Scaringe, R. P.; Stojakovic, D. R.; Hoffman, B. M.; Ibers, J. A.; Marks, T. J. *J. Am. Chem. Soc.* **1980**, *102*, 6702–6713.

(4) For conductive cofacial polymers with other types of metallomacrocycles or bridging groups, see: (a) Hanack, M. *GIT Fachz. Lab.* **1987**, *2*, 75–78, and references therein. (b) Hanack, M.; Deger, S.; Keppeler, U.; Lange, A.; Leverenz, A.; Rein, M. In ref 1a, *19*, 739–744, and references therein. (c) Collman, J. P.; McDevitt, J. T.; Leidner, C. R.; Yee, G. T.; Torrance, J. B.; Little, W. A. *J. Am. Chem. Soc.* **1987**, *109*, 4606–4614. (d) Wynne, K. J. *Inorg. Chem.* **1985**, *24*, 1339–1343, and references therein. (e) Diel, B. N.; Inabe, T.; Jaggi, N. K.; Lyding, J. W.; Schneider, O.; Hanack, M.; Kannewurf, C. R.; Marks, T. J.; Schwartz, L. H. *J. Am. Chem. Soc.* **1984**, *106*, 3207–3214. (f) Moyer, T. J.; Schechtman, L. A.; Kenney, M. E. *Polym. Prepr.* **1984**, *25*, 234–235. (g) Hanack, M. *Chimia* **1983**, *37*, 238–245. (h) Nohr, R. S.; Kuznesof, P. M.; Wynne, K. J.; Kenney, M. E.; Siebenman, P. G. *J. Am. Chem. Soc.* **1981**, *103*, 4371–4377. (i) Orthmann, E. A.; Enkelmann, V.; Wegner, G. *Makromol. Chem., Rapid Commun.* **1983**, *4*, 687–692.

(5) (a) Dirk, C. W.; Inabe, T.; Schoch, K. F., Jr.; Marks, T. J. *J. Am. Chem. Soc.* **1983**, *105*, 1539–1550. (b) Diel, B. N.; Inabe, T.; Lyding, J. W.; Schoch, K. F., Jr.; Kannewurf, C. R.; Marks, T. J. *J. Am. Chem. Soc.* **1983**, *105*, 1551–67.

(6) (a) Doris, K. A.; Ciliberto, E.; Fragalà, I.; Ratner, M. A.; Marks, T. J. In ref 1d, pp 337–346. (b) Pietro, W. J.; Marks, T. J.; Ratner, M. A. *J. Am. Chem. Soc.* **1985**, *107*, 5387–5391. (c) Pietro, W. J.; Ellis, D. E.; Marks, T. J.; Ratner, M. A. *Mol. Cryst. Liq. Cryst.* **1984**, *105*, 273–287. (d) Ciliberto, E.; Doris, K. A.; Pietro, W. J.; Reisner, G. M.; Ellis, D. E.; Fragalà, I.; Herbstein, F. H.; Ratner, M. A.; Marks, T. J. *J. Am. Chem. Soc.* **1984**, *106*, 7748–7761. (e) Hale, P. D.; Pietro, W. J.; Ratner, M. A.; Ellis, D. E.; Marks, T. J. *J. Am. Chem. Soc.* **1987**, *109*, 5943–5947.

(7) (a) Inabe, T.; Gaudiello, J. G.; Moguel, M. K.; Lyding, J. W.; Burton, R. L.; McCarthy, W. J.; Kannewurf, C. R.; Marks, T. J. *J. Am. Chem. Soc.* **1986**, *108*, 7595–7608. (b) Gaudiello, J. G.; Marcy, H. O.; McCarthy, W. J.; Moguel, M. K.; Kannewurf, C. R.; Marks, T. J. *Synth. Met.* **1986**, *15*, 115–128. (c) Inabe, T.; Moguel, M. K.; Marks, T. J.; Burton, R.; Lyding, J. W.; Kannewurf, C. R. *Mol. Cryst. Liq. Cryst.* **1985**, *118*, 349–352. (d) Inabe, T.; Kannewurf, C. R.; Lyding, J. W.; Moguel, M. K.; Marks, T. J. *Mol. Cryst. Liq. Cryst.* **1983**, *93*, 355–367.

(8) Preliminary reports: (a) Almeida, M.; Gaudiello, J. G.; Marks, T. J.; Butler, J. C.; Marcy, H. O.; Kannewurf, C. R. *Synth. Met.* **1987**, *21*, 261–266. (b) Gaudiello, J. G.; Almeida, M.; Marks, T. J.; McCarthy, W. J.; Butler, J. C.; Kannewurf, C. R. *J. Phys. Chem.* **1986**, *90*, 4917–4920.

(9) For the semiconductor $(NMP)_x(Phen)_{1-x}(TCNQ)$, NMP = *N*-methylphenazine, Phen = phenazine, ρ has been tuned from ca. -0.50 to -0.66 in the TCNQ-based band: (a) Miller, J. S.; Epstein, A. J. *Angew. Chem., Int. Ed. Engl.* **1987**, *26*, 287–293. (b) Epstein, A. J.; Miller, J. S.; Pouget, J. P.; Comès, R. *Phys. Rev. Lett.* **1981**, *47*, 741–744.

(10) (a) Roth, S.; Bleier, H. *Adv. Phys.* **1987**, *36*, 385–462. (b) Skotheim, T. A., Ed. *Handbook of Conducting Polymers*; Marcel Dekker: New York, 1986; Vol. 1, 2. (c) Frommer, J. E.; Chance, R. R. In *Encyclopedia of Polymer Science and Engineering*; Wiley: New York, 1986; Vol. 5, pp 462–507. (d) Wynne, K. J.; Street, G. B. *Ind. Eng. Chem. Prod. Res. Dev.* **1982**, *21*, 23–28. (e) Baughman, R. H.; Brédas, J. L.; Chance, R. R.; Elsenbaumer, R. L.; Shacklette, L. W. *Chem. Rev.* **1982**, *82*, 209–222. (f) Wegner, G. *Angew. Chem., Int. Ed. Engl.* **1981**, *20*, 361–381.

(11) (a) Diaz, A. F.; Bargon, J. In ref 10b, Vol. 1, Chapter 3, pp 81–115. (b) Tourillon, G. *Ibid.*; Chapter 9, pp 293–350. (c) MacDiarmid, A. G.; Kaner, R. B. *Ibid.*; Chapter 20, pp 689–727. (d) Murray, R. W. In *Electroanalytical Chemistry*; Bard, A. J., Ed.; Marcel Dekker, Inc.: New York, 1984; Vol, 13, pp 191–368.

(12) Alameida, M.; Gaudiello, J. G.; Kellogg, G. E.; Tetrick, S. M.; Marcy, H. O.; McCarthy, W. J.; Butler, J. C.; Kannewurf, C. R.; Marks, T. J. *J. Am. Chem. Soc.*, following paper in this issue.

(13) Walter, M.; Ramaley, L. *Anal. Chem.* **1973**, *45*, 165–166.

Molecular Metals with Widely Tunable Band Filling

J. Am. Chem. Soc., Vol. 111, No. 14, 1989 5261

Synthesis of Tetragonal [Si(Pc)O]$_n$. The tetragonal polytype of [Si-(Pc)O]$_n$ was obtained either by electrochemically undoping {[Si(Pc)-O](BF$_4$)$_{0.50}$}$_n$ (vide infra) or, in larger quantities, by thermally undoping chemically prepared {[Si(Pc)O](I$_3$)$_{0.36}$}$_n$. The iodine-doped material was prepared by stirring orthorhombic [Si(Pc)O]$_n$ in benzene with I$_2$ as previously described.[5b] To prepare pure undoped tetragonal[Si(Pc)O]$_n$, the iodine-doped material (tetragonal {[Si(Pc)O](I$_3$)$_{0.36}$}$_n$) was initially washed with benzene to remove unreacted I$_2$. The finely ground doped polymer was then heated in a tube furnace to 400 °C under dynamic vacuum (10^{-4} Torr) for 12 h. The thermal undoping procedure (i.e., mortar and pestle grinding and heating under vacuum) was carried out a total of three times to ensure the complete removal of the iodine. The residual doping level/iodine content after this treatment was monitored by infrared spectroscopy, X-ray powder diffraction, and elemental analysis and was typically less than 0.01% I, i.e., a degree of partial oxidation of less than 0.002 (based on I$_3$$^-$).

Preparation of Tetra-n-butylammonium Hexafluoroantimonate. Tetra-n-butylammonium hexafluoroantimonate, (n-Bu$_4$N$^+$)SbF$_6$$^-$, was prepared by a modification of the literature procedure.[14] An acetonitrile solution of NaSbF$_6$ (5.00 g, 20.0 mmol in 125 mL) and AgNO$_3$ (3.33 g, 20.0 mmol in 30 mL) was stirred in a flask wrapped with aluminum foil for ~1 h. The NaNO$_3$ precipitate was removed by filtration, and the colorless filtrate containing AgSbF$_6$ was then reacted with an acetonitrile solution of (n-Bu$_4$N$^+$)I$^-$ (7.50 g, 20.0 mmol in 50 mL). The resulting AgI precipitate was removed by centrifugation. Under vacuum, the supernatant solution was slowly reduced in volume to ca. 50 mL. Addition of water (100 mL) then precipitated (n-Bu$_4$N$^+$)SbF$_6$$^-$ as a white powder. This solid was isolated by filtration and was washed several times with cold water. The crude product was recrystallized three times from hot ethanol and the white crystalline solid dried in vacuo overnight: yield 3.0 g (64%); IR (Nujol mull) shows a ν(Sb–F) stretch at 660 cm^{-1}.[14] Anal. Calcd for C$_{16}$H$_{36}$NF$_6$Sb: C, 40.19; H, 7.59; F, 23.84. Found: C, 40.27; H, 7.15; F, 22.73.

Preparation of Tetra-n-butylammonium Nonafluoro-n-butanesulfonate. This salt was prepared by metathesis of potassium nonafluoro-n-butanesulfonate with tetra-n-butylammonium hydroxide in water. The potassium salt (15.0 g, 45.0 mmol in 275 mL of H$_2$O) was mixed with 50 mL of 1 M (n-Bu$_4$N$^+$)OH$^-$ (electrometric grade, Southwestern Analytical). A colorless oil immediately formed and settled to the bottom of the flask. The oil was isolated by centrifugation and dried in air to yield a white crystalline solid. The solid, obtained in essentially quantitative yield, was washed with cold heptane and dried in vacuo. Anal. Calcd for C$_{20}$H$_{36}$NF$_9$SO$_3$: C, 44.36; H, 6.70; F, 31.57. Found: C, 44.52; H, 6.56; F, 31.38.

Preparation of Tetra-n-butylammonium 1-Pyrenesulfonate. This salt was prepared by a modification of the 1-pyrenesulfonic acid synthesis of Menger and Whitesell.[15] Pyrene (15.0 g, 24.0 mmol) in 60 mL of nitrobenzene was treated dropwise with concentrated H$_2$SO$_4$ (12.0 mL, 215 mmol), which resulted in a greenish-yellow precipitate. This solid (1-pyrenesulfonic acid) was collected by suction filtration, washed with ca. 250 mL of benzene to remove unreacted pyrene, and then dried in vacuo. The acid was then dissolved in H$_2$O and reprecipitated with concentrated HCl. A second reprecipitation was next accomplished from hot concentrated HCl. The resulting solid (wet, ca. 30 g) was dissolved in 100 mL of hot H$_2$O and reacted with 60 g of 40% (n-Bu$_4$N$^+$)OH$^-$ in H$_2$O. A greenish-yellow oil formed immediately, which yielded a greenish-yellow solid on cooling. This was washed with H$_2$O on a frit and dried in vacuo. The salt, (n-Bu$_4$N$^+$)PYS$^-$, was recrystallized twice from acetone/ether. Cyclic voltammetry of this salt shows an irreversible oxidation at ca. 1.05 V vs SSCE. Doping experiments using (n-Bu$_4$N$^+$)PYS$^-$ as the electrolyte were carried out at potentials lower than 1.0 V. Anal. Calcd for C$_{32}$H$_{45}$NO$_3$S: C, 73.38; H, 8.66; S, 6.12. Found: C, 73.24; H, 8.80; S, 6.35.

Preparation of Tetra-n-butylammonium Sulfate. Under light-free conditions thallium sulfate (3.59 g, 71.1 mmol) in 750 mL of water was added dropwise with stirring to a 750-mL solution of (n-Bu$_4$N$^+$)I$^-$ (50.0 g, 135 mmol), resulting in immediate precipitation of TlI. This mixture was stirred for ca. 16 h before TlI was removed by suction filtration. The colorless aqueous filtrate was then reduced to approximately 50 mL in vacuo. Care must be taken not to heat the solution above 50 °C, as total decomposition occurs at approximately 90 °C. This solution was then filtered again to remove ca. 0.1 g of TlI. Removing the remaining H$_2$O in vacuo left an off-white waxy material which was dried for 12 h under high vacuum. Next, 50 mL of CH$_2$Cl$_2$ was vacuum transferred onto the crude product, leaving ca. 0.3 g of undissolved Tl$_2$SO$_4$, which was removed by filtration. The methylene chloride was then removed in vacuo yielding (n-Bu$_4$N$^+$)$_2$SO$_4$$^{2-}$ as a colorless waxy solid. To ensure complete
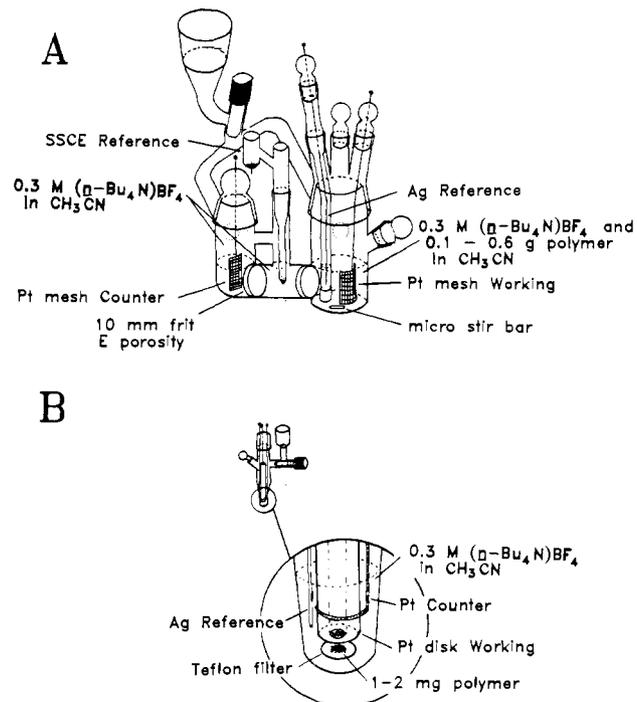
Figure 1. Schematic diagrams of electrochemical cells for (A) slurry doping experiments and (B) microcompaction doping experiments.

dryness, the material was subjected to repeated dissolution in a 1:1 acetonitrile/benzene mixture (which forms an 8% azeotrope with water at atmospheric pressure) followed by solvent removal in vacuo. Anal. Calcd for C$_{32}$H$_{72}$N$_2$O$_4$S: C, 66.15; H, 12.49; N, 4.81; S, 5.52. Found: C, 66.77; H, 12.49; N, 4.64; S, 5.35.

Electrochemical Instrumentation. Electrochemical measurements were performed on a EG&G Princeton Applied Research Model 273 potentiostat/galvanostat interfaced to a Zenith ZF-158 (XT-type) microcomputer via an IEEE-488 (GPIB) interface (National Instruments GPIB-PC2A). Locally developed BASIC programs controlled the operation of the potentiostat for cyclic voltammetry, controlled-potential coulometry, and electrochemical potential spectroscopy experiments.

Electrochemistry. Purities of the electrochemical solvents and supporting electrolytes were monitored by cyclic voltammetry. Thus, the usable oxidation window of each electrolyte was determined before use in bulk electrolysis experiments. Two types of electrochemical doping experiments were performed: macroscopic preparative-scale slurry doping experiments in a standard three-compartment cell with a large-area (ca. 8 cm^2) platinum gauze working electrode; and microcompaction doping experiments employing a composite electrode constructed from a platinum disk electrode. Schematic depictions of the two approaches are shown in Figure 1. The electrochemical solutions for the slurry doping bulk electrolysis experiments (Figure 1A) were prepared by vacuum transferring the solvent directly into the three-compartment cell containing the dry supporting electrolyte (0.3 M) and a known amount (ca. 0.100–0.600 g) of the [Si(Pc)O]$_n$ polymer or Ni(Pc) molecular phthalocyanine. The microcompaction experiments (Figure 1B) were performed with a composite working electrode: a platinum disk pressed against a small (ca. 1–2 mg) portion of finely ground [Si(Pc)O]$_n$ that was placed on a circular Teflon filter membrane (Zitex, 2–5 or 10–20 μm mean pore size) and held firmly against the Pt surface with perforated Teflon tape or a Teflon-coated O-ring. This composite electrode was studied in a single-compartment cell using 0.5–1.0 mL of a 0.3 M acetonitrile solution of supporting electrolyte. This methodology is similar to that recently described by Collman et al.,[4c] who employed a carbon (graphite) cloth as an electrode for electrochemical studies of insoluble macrocyclic polymers. Orthmann et al. galvanostatically oxidized [Si-(Pc)O]$_n$ by pressing the polymer against a glass frit with a graphite foil electrode.[4i] Similarly, metal chalcogenide electrochemical experiments are commonly performed on a mixture of the chalcogenide material and Teflon pressed onto a platinum mesh electrode.[16a,b] Silver wire quasireference electrodes (AgRE) used during the present experiments were referenced directly to a sodium-saturated calomel electrode (SSCE) at

---

(14) Qureshi, A. M.; Aubke, F. *Can. J. Chem.* **1970**, *48*, 3117.

(15) Menger, F. M.; Whitesell, L. G. *J. Org. Chem.* **1987**, *52*, 3793–3798.

(16) (a) Whittingham, M. S. *J. Solid State Chem.* **1979**, *29*, 303–310. (b) Schöllhorn, R.; Kümpers, M.; Besenhard, J. O. *Mater. Res. Bull.* **1977**, *12*, 781–788.

the completion of the experiments. Control studies utilizing an SSCE reference during the entire course of the experiment verified that drift of the AgRE was negligible. All potentials in this work are reported vs the SSCE reference. After solvent transfer, the cells were backfilled with an atmosphere of argon. For the macroscopic slurry doping experiments, the doped polymer was isolated and the supporting electrolyte removed by repeated centrifugation in acetonitrile. Dopant levels (degree of partial oxidation, y, i.e., $\{[Si(Pc)O]X_y\}_n$) were determined by both elemental analyses and coulometry: eq 1,[17] where $Q°$ is the gross coulombs

$$y = (Q° - i_b t)/N_o F \qquad (1)$$

measured, i_b is the final background current, t is the elapsed time of experiment, N_o is the moles of $[Si(Pc)O]_n$ based on monomer molecular weight, and F is Faraday's constant. Coulometric and analytical results agreed to better than $\pm 3\%$ ($\Delta y = \pm 0.03$).

Electrochemical Potential Spectroscopy (ECPS) experiments were performed by a method somewhat different from that described by Thompson.[18] Following a potential step, current decay was monitored until a steady-state condition was achieved, i.e., di/dt approaching zero, rather than using a preset minimum current as the convergence criterion. This method was preferable because the background current was found *not* to be independent of the applied potential. Typical convergence criteria used were 5×10^{-10} A cm^{-2} s^{-1} for the microcompaction doping experiments and 4.2×10^{-11} A cm^{-2} s^{-1} for slurry doping experiments. At these limits, the contribution of nonfaradaic charge (background) to the total charge passed is less than 10%. When this current decay criterion was met five times, the i vs t data were stored and the next set potential was automatically applied.

Exploratory reductive doping experiments on tetragonal $[Si(Pc)O]_n$ were carried out in the microcompaction mode described above. The supporting electrolyte was $(n\text{-}Bu_4N^+)BF_4^-/THF$. To quantitate the degree of $[Si(Pc)O]_n$ reduction, the microcompaction was initially oxidized to a potential where the degree of oxidation (y) had previously been established. The Coulombic scale for oxidation was then assumed to extrapolate linearly to the reductive regime.

Approximate diffusion coefficients for the electrochemical doping of the tetragonal $[Si(Pc)O]_n$ with the BF_4^- counterion were determined by chronopotentiometric[19,20] and chronocoulometric[21,22] methods. The working electrodes for these experiments were the small microcompaction composite electrodes described above. They were examined after an initial oxidation/reduction cycle. For experiments using the chronopotentiometric method, the voltage decay (to open circuit voltage) was monitored after $\tau = 100$ ms current pulses of ± 2 to ± 20 μA were applied. The voltage decay showed reasonably linear behavior vs $t^{-0.5}$ for $t = 0.1$–20 s, and the slopes were taken to be proportional to $D^{-0.5}$ (eq 2).

$$E = E_0 = \frac{i\tau RT}{C_o(nF)^2 A(\pi t D)^{0.5}} \qquad (2)$$

The constants R, T, C_o, and F are the gas low constant, temperature, initial electrolyte concentration, and the Faraday constant, respectively. The area, A, was assumed to be the area of the Pt disk electrode (0.08 cm^2). Diffusion coefficients ranging between 2.2×10^{-15} and 2.4×10^{-14} cm^2/s were estimated for the oxidative doping of tetragonal $[Si(Pc)O]_n$ using this method and data from a series of variable current experiments on the same electrode.

Chronocoulometrically determined diffusion coefficients were obtained via a Fick's law analysis[22] of controlled-potential coulometry data (eq 3).

$$L = (Dt)^{0.5} \qquad (3)$$

Here L is the diffusion length of the particle, taken to be the average particle radius, and t is the diffusion time. Crystallite dimensions were estimated to be $0.14 \times 0.014 \times 0.014$ μm based on BET surface area measurements and SEM data on crystallite shapes.[23] The diffusion time

is the time required to fully dope the polymer. It is identified as a sharp change in slope on a log–log plot of cumulative charge vs elapsed time. A typical diffusion coefficient estimate for the oxidative doping of tetragonal $[Si(Pc)O]_n$ is 3.7×10^{-14} cm^2/s from chronocoulometry. Measured diffusion coefficients were independent of the membrane mean pore size, thus arguing that diffusion through the membrane does not contribute to the reported coefficients.

X-ray Diffraction. X-ray powder diffraction data for all compounds studied were acquired on a Rigaku Geigerflex recording powder diffractometer, using Ni-filtered Cu Kα radiation. The powders were pressed (ca. 10 tons) into cylindrical pellets 13 mm in diameter and 1–2 mm thick. This pressing method has been shown to not produce pellets with significant preferential $\{[Si(Pc)O]X_y\}_n$ crystallite orientations.[5a] All data were recorded at a scanning rate of 0.50° min^{-1}. The receiving slit was set at 0.6 mm and the divergence and scattering slits were set at 0.5° for 5° < 2θ < 20°, at 1° for 20° < 2θ < 40°, and at 2° for 40° < 2θ < 60°. The apparatus was calibrated with Si powder[5a] as an internal standard for detailed studies of lattice parameters as a function of doping level.

Infrared Spectroscopy. Infrared spectra were recorded on a Nicolet Model 7199 Fourier transform instrument. Samples for FTIR spectroscopy were prepared as KBr wafers on a ring press (ca. 10 tons). The foreground (sample) signal was scanned 500 times and the background (air) signal was scanned 250 times before each was transformed and ratioed.

Results

The synthesis and structural characterization (X-ray diffraction, spectroscopic) of as-polymerized (orthorhombic) $[Si(Pc)O]_n$ ($n > 100$) have been discussed in detail elsewhere.[5a] The present discussion first focuses upon oxidative electrochemical doping phenomenology (removal of charge, insertion of a counterion) involving this material and the accompanying crystal structural changes as probed by X-ray diffraction. These results are then contrasted with the greatly different electrochemical behavior of a new, tetragonal polytype of $[Si(Pc)O]_n$. It is also shown that tetragonal $[Si(Pc)O]_n$ can be reversibly doped reductively. Evidence for homogeneous tunability of y for a number of X^- anions in $\{[Si(Pc)O]X_y\}_n$ materials is next presented. A detailed stoichiometric/diffractometric investigation of limiting y values is then presented for a range of structurally different X^- ions. These observations are shown to differ greatly from the electrochemical behavior of $[Ge(Pc)O]_n$. Finally, we inquire as to the significance of the siloxane backbone in $[Si(Pc)O]_n$ structural/redox phenomenology via a comparative study of Ni(Pc) electrochemistry. The differences are both marked and instructive.

Electrochemical Syntheses of $\{[Si(Pc)O]X_y\}_n$ Materials. General Remarks. The insolubility of $[Si(Pc)O]_n$ in conventional organic solvents and its markedly polycrystalline morphology necessitated the use of nonstandard approaches for the electrochemical doping of this polymer. For preparative-scale experiments, $[Si(Pc)O]_n$ was doped as a slurry. In this procedure (Figure 1A), a measured quantity of finely ground polymer is suspended in a vigorously stirred solution of acetonitrile/supporting electrolyte in one compartment of an anaerobic three-compartment cell. The potential of the working electrode is then poised (vs an Ag quasi-reference electrode) at a preselected value (vide infra) and the resulting current measured as a function of time. This variant of controlled-potential coulometry (CPC)/bulk electrolysis,[17] permits gram-scale electrochemical doping of $[Si(Pc)O]_n$ and the isolation of pure macroscopic samples of a given level of oxidation suitable for additional chemical and physical characterization. Smaller scale doping experiments were carried out on microcompactions. Here (Figure 1B), a small sample of polymer is placed on a Teflon filter membrane that is pressed against the platinum disk working electrode and held in place with Teflon tape. This electrode is then studied in a single-compartment cell containing only solvent and supporting electrolyte. This procedure produces only a small quantity of doped material, but has the advantages of a more rapid response time (ca. 10 times faster than the slurry method) and a methodology directly comparable to more

(17) (a) Bard, A. J.; Faulkner, L. R. *Electrochemical Methods. Fundamentals and Applications*; Wiley: New York, 1980. (b) Zuman, P. *Microchem. J.* **1987**, *36*, 255–284.

(18) Thompson, A. H. *Rev. Sci. Instrum.* **1983**, *54*, 229–237.

(19) Will, F. G. *J. Electrochem. Soc.* **1985**, *132*, 2093–2099.

(20) Winn, D. A.; Shemilt, J. M.; Steele, B. C. H. *Mater. Res. Bull.* **1976**, *11*, 559–566.

(21) Reference 17a, pp 199–206.

(22) Kiess, H.; Meyer, W.; Baeriswyl, D.; Harbeke, G. *J. Electron. Mater.* **1980**, *9*, 763–781.

(23) (a) Kellogg, G. E.; Gillespie, R.; Marks, T. J., unpublished data. (b) Larger crystallite dimensions ($2.0 \times 0.2 \times 0.2$ μm) were observed for $[Ge(Pc)O]_n$ by SEM.[24]

(24) (a) Zhou, X.; Marks, T. J.; Carr, S. H. *J. Polym. Sci., Polym. Phys. Ed.* **1985**, *23*, 305–313. (b) Zhou, X.; Marks, T. J.; Carr, S. H. *Polymeric Mater. Sci. Eng.* **1984**, *51*, 651–654.

conventional electrochemical doping/intercalation experiments with polyacetylene[10,11,25] and metal chalcogenides.[18,20,26] Results using slurry and microcompaction techniques are qualitatively in agreement.

Following a potential step, the current vs time data for the slurry doping of orthorhombic $[Si(Pc)O]_n$ reveal an exponential decay to a constant background level, and except for a small increase in current at early times (vide infra) and the time scale of the electrolysis, the response is reminiscent of CPC behavior observed for soluble species undergoing a simple redox process.[17a] Whereas typical solution CPC experiments require on the order of 1 h to complete, the gram-scale slurry oxidation of $[Si(Pc)O]_n$ requires 18–36 h per oxidation level (y). The increased electrolysis time can be attributed to a slower rate of mass transfer of the insoluble $[Si(Pc)O]_n$ particles to the electrode. The initial rise in current observed from $t \approx 0$–100 s appears to reflect both a percolation-like increase in doping rate as the initially poorly conductive sample becomes more conductive[5b,7a] and the overcoming of structural barriers to doping as the material rearranges to the more facilely doped tetragonal crystal structure of the product (vide infra). Support for the latter contention is provided by doping experiments with tetragonal $[Si(Pc)O]_n$ (vide infra) in which the current begins ($t > 0$) at a high level and no rise is observed.

The current vs time profiles in microcompaction doping experiments with orthorhombic $[Si(Pc)O]_n$ are qualitatively similar to those observed for the slurry doping, including the small increase in current at early times. Two major differences are smaller currents and more rapid time response. The first difference is attributable to the smaller sample size, while the second is most likely due to the closer polymer–electrode contact and the consequently more efficient charge transfer. Slurry doping experiments on small amounts (ca. 0.025 g) of $[Si(Pc)O]_n$ are not significantly faster than those on larger samples, indicating that the response time is essentially independent of sample size. Likewise, i vs t profiles are insensitive to the extent of sample grinding (particle sizes over a range of 5–30 μm by SEM) in both slurry and microcompaction experiments. Phenomenological diffusion coefficients for electrochemical doping of tetragonal $[Si(Pc)O]_n$ were estimated by both chronopotentiometric[19,20] and chronocoulometric[21,22] techniques in 0.2 M $(n\text{-}Bu_4N^+)BF_4^-/CH_3CN$ (see Experimental Section for details). Diffusion coefficients in the range 10^{-13}–10^{-15} cm^2/s are estimated, which are in the general range reported for other conductive polymers.[10,11,22,25] In contrast, coefficients for Li$^+$ insertion into typical transition-metal chalcogenides are several orders of magnitude greater.[20,26]

Doping of Orthorhombic $[Si(Pc)O]_n$. Electrochemical Potential Spectroscopy and Structural Aspects. While the aforementioned CPC procedures provide a synthetic route to $\{[Si(Pc)O]X_y\}_n$ materials of a given y, far more information on kinetic, structural, and thermochemical aspects of the doping process is provided by electrochemical potential spectroscopy (ECPS) experiments[18] (also known as EVS—electrochemical voltage spectroscopy).[25e,f] The ECPS experiment consists of a series of sequential CPC experiments in which the applied potential is incrementally varied. At each set point on a potential ramp, the current decay as a function of time is measured (see Experimental Section for details) and
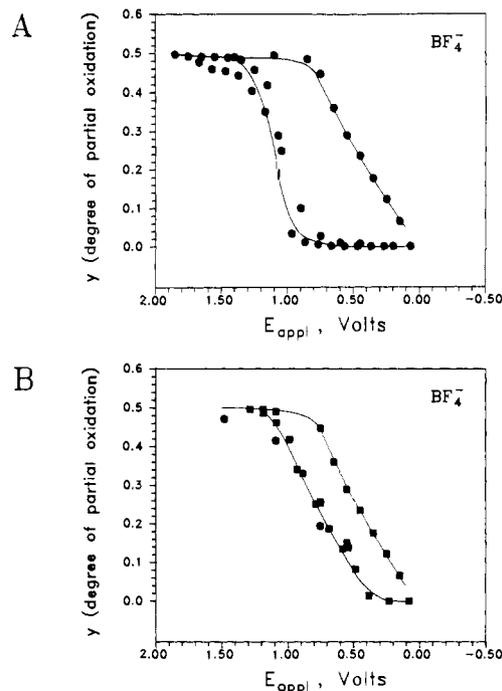
Figure 2. Electrochemical potential spectroscopy (ECPS) plot for slurry doping of (A) orthorhombic $[Si(Pc)O]_n$ in $(n\text{-}Bu_4N^+)BF_4^-$/acetonitrile and (B) tetragonal $[Si(Pc)O]_n$ in $(n\text{-}Bu_4N^+)BF_4^-$/acetonitrile.

the net charge passed at that potential is recorded. The degree of partial oxidation (y) is then the net charge passed normalized for the number of moles of polymer repeat units. Plotting y as a function of E_{appl} then yields a standard ECPS plot. Importantly, abrupt steps in ECPS plots are diagnostic of transitions between discrete phases of differing crystal structure and/or stoichiometry.[18,25,26] The following discussion focuses upon correlated ECPS and X-diffractometric studies of orthorhombic $[Si(Pc)O]_n$.

Figure 2A shows the ECPS curve obtained for the slurry doping of orthorhombic $[Si(Pc)O]_n$ in $(n\text{-}Bu_4N^+)BF_4^-$/acetonitrile. Electrochemical doping of the as-polymerized (orthorhombic) polymer occurs initially at about 1.0–1.2 V vs SSCE[27a] and is marked by a fairly sharp discontinuity (steep slope) in y (degree of partial oxidation) at this potential. At 1.3–1.5 V, y reaches a stable plateau at approximately 0.50 electrons per Si(Pc)O unit, i.e., 0.5 hole per site. Potentials greater than 2.4 V (not shown) result in an irreversible oxidation process corresponding to destruction of the polymer.[27b] Undoping the $\{[Si(Pc)O](BF_4)_{0.50}\}_n$ product (i.e., reversed cycling to less positive applied potentials) begins at ca. 0.90 V and proceeds smoothly to $y = 0.00$ at E_{appl} of 0.00 to -0.10 V. Infrared spectroscopic data (vide infra), elemental analysis, and charge-transport results[12] also indicate that the material is completely undoped at this point. The steep slope of the ECPS curve for oxidation at E_{appl} of 1.0–1.2 V vs SSCE suggests a significant structural reorganization.[18,25,26] X-ray diffraction results lend further support to this hypothesis (vide infra). The plateau at $y \approx 0.50$ is a surprising result in light of the fact that $y = 0.36$ (3) was the maximum degree of partial oxidation observed with NO^+X^- or halogen *chemical* oxidants.[5,7] The rationale for this observation will be a focus of the Discussion. A third notable feature of Figure 2 is the smooth return portion of the curve, i.e., for decreasing E_{appl}. This suggests that there is *not* a major structural/phase transformation upon reduction

(25) (a) Shacklette, L. W.; Toth, J. E.; Murthy, N. S.; Baughmann, R. H. *J. Electrochem. Soc.* **1985**, *132*, 1529–1535. (b) Shacklette, L. W.; Murthy, N. S.; Baughmann, R. H. *Mol. Cryst. Liq. Cryst.* **1985**, *121*, 201–209. (c) Maxfield, M.; Mu, S. L.; MacDiarmid, A. G. *J. Electrochem. Soc.* **1985**, *132*, 838–841. (d) Shacklette, L. W.; Toth, J. E. *Phys. Rev. B* **1985**, *32*, 5892–5901. (e) Kaufman, J. H.; Kaufer, J. W.; Heeger, A. J.; Kaner, R.; MacDiarmid, A. G. *Phys. Rev. B* **1982**, *26*, 2327–2330. (f) Kaufman, J. H.; Chung, T.-C.; Heeger, A. J. *J. Electrochem. Soc.* **1984**, *131*, 2847–2856. (g) Kaner, R. B.; MacDiarmid, A. G. *J. Chem. Soc., Faraday Trans. 1* **1984**, *80*, 2109–2118.

(26) (a) Rouxel, J.; Brec, R. *Annu. Rev. Mater. Sci.* **1986**, *16*, 137–162. (b) Betz, G.; Tributsch, H. *Prog. Solid State Chem.* **1985**, *16*, 195–290. (c) Huang, C.-K.; Crouch-Baker, S.; Huggins, R. A. *J. Electrochem. Soc.* **1988**, *135*, 408–412. (d) Huan, G.; Greenblatt, M. *Mater. Res. Bull.* **1987**, *22*, 505–512. (e) Yamamoto, T.; Kikkawa, S.; Koizumi, M. *Solid State Ionics* **1985**, *17*, 63–66. (f) Whittingham, M. S. *Ann. Chim. (Paris)* **1982**, *7*, 204–214. (g) Whittingham, M. S. *Prog. Solid State Chem.* **1978**, *12*, 41–99.

(27) (a) In earlier communications,[8] initial oxidation of the orthorhombic polytype was reported to occur at ca. 1.6 V vs SSCE. With our improved instrumentation, i.e., computer control of the ECPS experiment, we find that the onset of doping occurs at a somewhat lower potential, ca. 1.0–1.2 V, and is (initially) a low-current process that was not detectable with earlier analog instrumentation. (b) Experiments in liquid SO_2 show no further reversible change in y for potentials as high as $+3.0$ V vs SSCE. Irreversible decomposition occurs at higher potentials: Schlueter, J. A.; Kellogg, G. E.; Marks, T. J., unpublished observations.

Table I. Crystallographic Data for Partially Oxidized Phthalocyanine Materials

compd	space gp[a]	Z	cell param, Å
[Si(Pc)O]$_n$[b]	*Ibam*	4	$a = 13.80\ (5)$
			$b = 27.59\ (5)$
			$c = 6.66\ (4)$
[Si(Pc)O]$_n$[c]	P4/mcc	2	$a = 13.69\ (5)$
			$c = 6.67\ (4)$
{[Si(Pc)O](I$_3$)$_{0.37}$}$_n$[d]	P4/mcc	2	$a = 13.97\ (5)$
			$c = 6.60\ (4)$
{[Si(Pc)O](BF$_4$)$_{0.36}$}$_n$[e]	P4/mcc	2	$a = 13.70\ (7)$
			$c = 6.58\ (4)$
{[Si(Pc)O](BF$_4$)$_{0.50}$}$_n$	(P4/mcc)	2	$a = 13.96\ (7)$
			$c = 6.66\ (4)$
{[Si(Pc)O](PF$_6$)$_{0.36}$}$_n$[e]	P4/mcc	2	$a = 13.98\ (6)$
			$c = 6.58\ (4)$
{[Si(Pc)O](PF$_6$)$_{0.47}$}$_n$[c]	(P4/mcc)	2	$a = 14.08\ (7)$
			$c = 6.63\ (4)$
{[Si(Pc)O](SbF$_6$)$_{0.36}$}$_n$[e]	P4/mcc	2	$a = 14.31\ (4)$
			$c = 6.58\ (4)$
{[Si(Pc)O](SbF$_6$)$_{0.41}$}$_n$[c]	(P4/mcc)	2	$a = 14.19\ (7)$
			$c = 6.61\ (4)$
{[Si(Pc)O](TOS)$_{0.67}$}$_n$[c,f]	(P4/mcc)	2	$a = 14.39\ (7)$
			$c = 6.64\ (4)$
{[Si(Pc)O](PYS)$_{0.22}$}$_n$[c,g]	(P4/mcc)	2	$a = 13.70\ (7)$
			$c = 6.65\ (4)$
{[Si(Pc)O](CF$_3$SO$_3$)$_{0.55}$}$_n$[c]	(P4/mcc)	2	$a = 13.99\ (7)$
			$c = 6.60\ (4)$
{[Si(Pc)O](SO$_4$)$_{0.095}$}$_n$[c]	(P4/mcc)	2	$a = 13.86\ (7)$
			$c = 6.67\ (4)$
{[Si(Pc)O](NFBS)$_{0.38}$}$_n$[c,h]	(P4/mcc)	2	$a = 14.37\ (7)$
			$c = 6.63\ (4)$
{[Si(Pc)O](PFOS)$_{0.26}$}$_n$[c,i]	(P4/mcc)	2	$a = 13.91\ (7)$
			$c = 6.61\ (4)$
β-Cu(Pc)[j,k]	P2$_1$/a	2	$a = 19.407$
			$b = 4.790$
			$c = 14.628$
			$\beta = 120.93°$
γ-Pt(Pc)[k,l]	P2$_1$/a	2	$a = 23.16$
			$b = 3.969$
			$c = 16.62$
			$\beta = 129.4°$
Ni(Pc)(I$_3$)$_{0.33}$[k,m]	P4/mcc	2	$a = 13.936\ (6)$
			$c = 6.488\ (3)$
Ni(Pc)(BF$_4$)$_{0.35}$[k,n]	P4/mcc	2	$a = 13.97\ (2)$
			$c = 6.48\ (1)$
Ni(Pc)(BF$_4$)$_{0.48}$[k,c]	P4/mcc	2	$a = 13.82\ (7)$
			$c = 6.48\ (4)$
Ni(Pc)(ClO$_4$)$_{0.40}$[k,o]	P4/mcc	2	$a = 13.957\ (3)$
			$c = 6.4672\ (9)$
Ni(Pc)(SbF$_6$)$_{0.50}$[k,p]	Pnc2	2	$a = 14.113\ (3)$
			$b = 28.710\ (2)$
			$c = 6.441\ (2)$

[a] Assignments for the electrochemically generated {[Si(Pc)O]X$_y$}$_n$ salts are by analogy to the previously indexed materials[5,7a] and single-crystal results. These materials were synthesized by using the tetragonal [Si(Pc)O]$_n$ starting material. They are denoted by parentheses around the space group assignment. [b] Reference 5a. [c] This work. [d] Reference 5b. [e] Reference 7a. [f] TOS = *p*-toluenesulfonate. [g] PYS⁻ = 1-pyrenesulfonate. Probably inhomogeneously doped (see text). [h] NFBS = nonafluoro-*n*-butanesulfonate. [i] PFOS = perfluoro-*n*-octa-nesulfonate. [j] Reference 33. [k] Single-crystal diffraction result. [l] Reference 36. [m] Reference 3g. [n] Reference 3c. [o] Reference 3a. [p] Reference 3f.

of the doped {[Si(Pc)O](BF$_4$)$_y$}$_n$ polymer to $y = 0.00$.

Detailed X-ray powder diffraction analyses argue that upon *chemically oxidizing* [Si(Pc)O]$_n$, there is a change in crystal structure from orthorhombic to tetragonal (Table I).[5a,7a] Powder patterns for as-polymerized [Si(Pc)O]$_n$ have been indexed via computer simulation techniques in a closely packed orthorhombic crystal structure (*Ibam*),[5a] while the chemically oxidized {[Si(Pc)O]X$_{0.36}$}$_n$ materials can be indexed in a tetragonal crystal structure[5b,7a] (*P4/mcc*) similar to single-crystal diffraction results for M(Pc)X$_{0.33}$ and H$_2$(Pc)X$_{0.33}$ compounds.[3] This change in structure is schematically illustrated in Figure 3. The connectivity of the polymer chains is not affected by this crystal structure
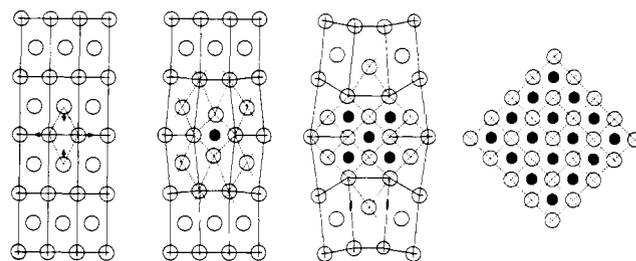
Orthorhombic ⟶ Tetragonal

Figure 3. Schematic illustration of the orthorhombic to tetragonal (doped) crystal structure change in [Si(Pc)O]$_n$. As depicted, the doping is inhomogeneous.
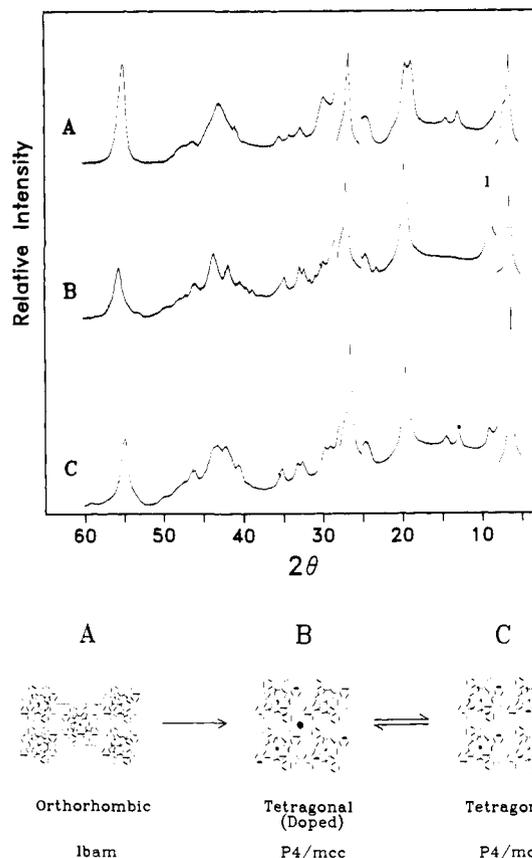
Figure 4. Top: X-ray diffraction data for polycrystalline samples of (A) as-polymerized (orthorhombic) [Si(Pc)O]$_n$, (B) {[Si(Pc)O](BF$_4$)$_{0.50}$}$_n$, and (C) electrochemically undoped (tetragonal) [Si(Pc)O]$_n$. Vertical scale settings in thousands of counts per second (kcps): 5–8°, 20 kcps; 8–25°, 4 kcps; 25–28°, 20 kcps; 28–60°, 4 kcps. Bottom: Crystal structure relationships in the electrochemistry of [Si(Pc)O]$_n$.

change, but the relative spatial arrangement of the [Si(Pc)O]$_n$ chains is altered to accommodate the inserted charge-compensating counterions. Note that this irreversible structural rearrangement may not be a particularly high-energy process—the actual nearest neighbor center-to-center Pc–Pc distances change only modestly: in the *Ibam* structure they are 15.24 [$^1/_2(a^2 + b^2)^{1/2}$] and 13.80 Å (*a*) apart,[5a] while in *P4/mcc* [for {[Si(Pc)O](BF$_4$)$_{0.36}$}$_n$] this distance is a uniform 13.70 Å (*a*).[7a]

Electrochemical doping of as-polymerized [Si(Pc)O]$_n$ also induces an orthorhombic → tetragonal structural transformation. Figure 4 presents diffraction data for orthorhombic [Si(Pc)O]$_n$, electrochemically doped {[Si(Pc)O](BF$_4$)$_{0.50}$}$_n$, and electrochemically undoped ($E_{appl} = -0.200$ V) polymer. The structure of the doped polymer is clearly rather similar to that observed for {[Si(Pc)O](BF$_4$)$_{0.36}$}$_n$ obtained by chemically oxidizing orthorhombic [Si(Pc)O]$_n$ with NO⁺BF$_4$⁻.[7a] The only significant dif-
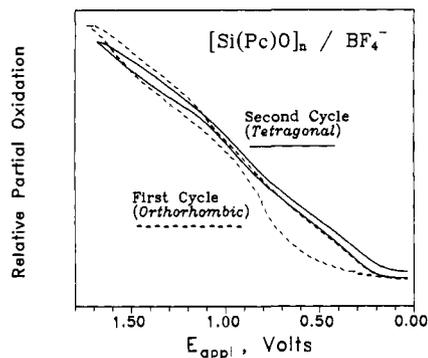
Figure 5. ECPS data for two cycles of microcompaction doping of orthorhombic $[Si(Pc)O]_n$ in $(n\text{-}Bu_4N^+)BF_4^-$/acetonitrile. The first cycle shows the characteristic discontinuity accompanying the orthorhombic $\rightarrow$ tetragonal structure change; the second and all succeeding cycles show electrochemical behavior characteristic of the tetragonal polytype.

Figure 6. X-ray diffraction data for polycrystalline samples of electrochemically doped tetragonal $\{[Si(Pc)O](BF_4)_y\}_n$ for (A) $y = 0.00$, (B) $y = 0.13$, (C) $y = 0.36$, and (D) $y = 0.50$. Vertical scale settings in thousands of counts per second (kcps): $5-8°$, 20 kcps; $8-25°$, 4 kcps; $25-28°$, 20 kcps; $28-60°$, 4 kcps.

ference in diffraction data is in the intensity of the reflections (most notably at $2\theta = 9°$) originating largely from electron density in the off-axis counterion channels.[5b,7a] The X-ray powder diffraction pattern of the electrochemically undoped $[Si(Pc)O]_n$ material (Figure 4C) is clearly dissimilar to the pattern obtained for the orthorhombic starting material (Figure 4A), especially in the $2\theta < 27°$ region. The similarity of the new $[Si(Pc)O]_n$ pattern (except at $2\theta = 9°$) to those of doped tetragonal $\{[Si(Pc)O]X_y\}_n$ compounds and to previous computer-generated data for tetragonal $(P4/m)$ $[M(Pc)O]_n$ trial structures[5a] argues that this new $[Si(Pc)O]_n$ structure is also tetragonal, i.e., extrusion of the BF_4^- anions during the electrochemical undoping process leaves the basic polysiloxane chain packing motif unaltered. Thus, electrochemical oxidation of as-polymerized orthorhombic $[Si(Pc)O]_n$ is accompanied by a major, diffractometrically detectable crystal structure change (a first-order structural phase transformation) and, as expected, a discontinuity in the ECPS profile (and $\{[Si(Pc)O](BF_4)_y\}_n$ stoichiometry[28]). In contrast, the ECPS data indicate that electrochemical undoping of tetragonal $\{[Si(Pc)O](BF_4)_{0.50}\}_n$ occurs smoothly over a broad potential (and stoichiometry) range with no evidence for major structural alterations. This assertion is strongly supported by the diffraction data.

Tetragonal $[Si(Pc)O]_n$. Synthesis and Electrochemical Potential Spectroscopy. In addition to the electrochemical synthesis described above, tetragonal $[Si(Pc)O]_n$ can also be prepared by thermally undoping tetragonal $\{[Si(Pc)O](I_3)_{0.36}\}_n$ (eq 4; see

$$\{[Si(Pc)O](I_3)_{0.36}\}_n \xrightarrow[\Delta]{-I_2} [Si(Pc)O]_n \qquad (4)$$
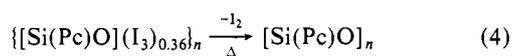
Experimental Section for details). The material made by this thermal procedure is infrared spectroscopically, diffractometrically, and electrochemically indistinguishable from that prepared electrochemically.

As can be seen in Figure 2B, the ECPS behavior of tetragonal $[Si(Pc)O]_n$ is considerably different from that of the orthorhombic phase. Thus, the onset of doping occurs at $+0.30$ to $+0.40$ V vs SSCE, and y as a function of E_{appl} is a smooth, linear function over a 0.90-V range up to ca. 1.20 V $(y = 0.50)$ where a plateau is reached analogous to that described for the orthorhombic polytype (Figure 2A). In addition, cycling back to lower potentials undopes the tetragonal material in a manner identical with undoping the oxidized orthorhombic polytype of $[Si(Pc)O]_n$ because the fully doped materials of both polytypes are spectroscopically, diffractometrically, magnetically,[12] and electrically[12] indistinguishable. One interesting feature of this curve is the significant hysteresis between the doping and undoping legs of the cycle. This appears to reflect the slow charge transfer associated with the
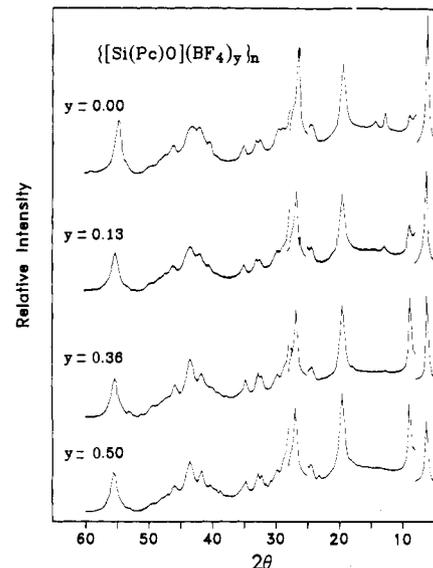
slurry experiment. Attempts to close the hysteresis in the slurry configuration by using an electrochemical mediator[29] such as $Os(bpy)_3^{2+}$ [30] were unsuccessful in that the profile of the y vs E_{appl} curves remained unchanged.

Further understanding of the relationship between the electrochemistry of the orthorhombic and tetragonal polytypes derives from microcompaction doping experiments. As shown in Figure 5, the initial ECPS response for orthorhombic $[Si(Pc)O]_n$ oxidized in $(n\text{-}Bu_4N^+)BF_4^-$ as the electrolyte (dashed line) is qualitatively similar to that obtained by slurry doping. After the resulting doped material is cycled back to $y = 0.00$, the polymer can be redoped at a lower initial potential, with a narrower hysteresis and smooth ECPS response reminiscent of that observed in slurry doping of tetragonal $[Si(Pc)O]_n$. In fact, all succeeding ECPS cycles on this microcompaction are identical with that of the second cycle, as are initial ECPS doping curves obtained on microcompactions prepared directly from the thermally or electrochemically prepared tetragonal polymer. The qualitative similarity between the ECPS results from the slurry and microcompaction electrode doping configurations includes the evident overpotential for doping orthorhombic $[Si(Pc)O]_n$. Differences between the two types of measurements, especially the smaller hysteresis between doping and undoping, can be reasonably attributed to mass transfer and electrode contact effects.

The aforementioned X-ray diffraction results confirm that there is an orthorhombic to tetragonal structural change when the polymer is oxidatively doped. The interesting result that the tetragonal structure is retained when the polymer is undoped either electrochemically or thermally also has consequences for the electrochemistry of the tetragonal polymer. One consequence is that the tetragonal $[Si(Pc)O]_n$ phase can be oxidized/counterions inserted at a much lower applied potential than for the orthorhombic phase. This difference of ca. 0.7 V in slurry electrochemistry is an example of poorly understood "break-in" phenomena observed in the electrochemistry of many conductive polymers.[31] The present results provide some of the most con-

---

(28) Attempts were also made to analyze products from orthorhombic $[Si(Pc)O]_n$ doping for E_{appl} at the steepest portion of the slurry ECPS plot (Figure 2A). X-ray diffraction showed that tetragonal $\{[Si(Pc)O]X_y\}_n$ material was present, indicating that structural rearrangement accompanied the passage of charge and that no obvious third phase was detectable.

(29) Szentrimay, R.; Yeh, P.; Kuwana, T. In *Electrochemical Studies of Biological Systems*; Sawyer, D. T., Ed. ACS Symposium Series 38 American Chemical Society: Washington, DC, 1977; pp 143–169.

(30) Malsumura-Inoue, T.; Tominaga-Morimoto, T. *J. Electroanal. Chem.* **1978**, *93*, 127–139.

(31) (a) Pickup, P. G.; Osteryoung, R. A. *J. Am. Chem. Soc.* **1984**, *106*, 2294–2299. (b) Kaufman, F. B.; Schroeder, A. H.; Engler, E. M.; Kramer, S. R.; Chambers, J. Q. *J. Am. Chem. Soc.* **1980**, *102*, 483–488.

A

B
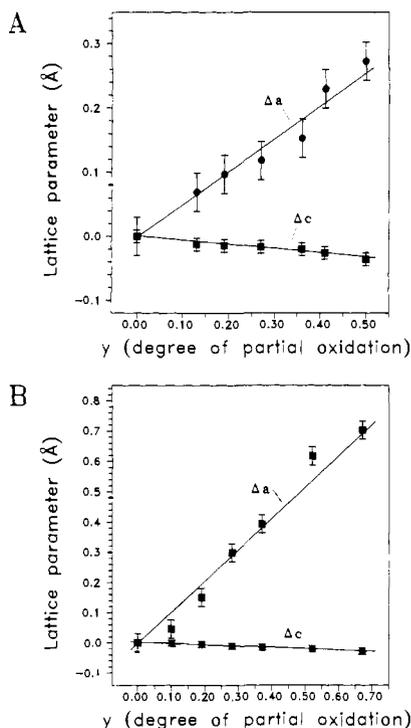
Figure 7. Change in lattice parameters as a function of degree of partial oxidation for (A) {[Si(Pc)O](BF$_4$)$_y$}$_n$ and (B) {[Si(Pc)O](TOS)$_y$}$_n$.

Figure 8. Transmission infrared spectra of {[Si(Pc)O](BF$_4$)$_y$}$_n$ as KBr wafers. The broad electronic absorption centered near 2000 cm^{-1} is characteristic of oxidized phthalocyanine conductors.

Figure 9. ECPS data for a tetragonal [Si(Pc)O]$_n$ microcompaction in (n-Bu$_4$N$^+$)BF$_4^-$/THF showing reversible reductive and oxidative doping. The anodic process is limited by the electrochemical window of THF.

vincing evidence to date that "break-in" effects are structural in origin. Another important observation in the tetragonal [Si(Pc)O]$_n$ ECPS data is the smooth, monotonic transformation from the undoped tetragonal polymer to the fully doped {[Si(Pc)O]-(BF$_4$)$_{0.50}$}$_n$ material (Figures 2B and 5). This behavior argues that the degree of partial oxidation (y) is a continuous function of E_{appl} for the tetragonal [Si(Pc)O]$_n$/BF$_4^-$ system and that the system is at the maximum y for each potential along the curve. Preparative experiments lend further support in that there is excellent agreement between coulometrically derived $y(E)$ values and those obtained by elemental analysis. The implication here is that materials isolated at intermediate potentials are *homogeneously doped*, and that they can be "tuned" to a desired level of band filling. Structural results (vide infra) demonstrate this point further.

Figure 6 presents diffraction data as a function of y for {[Si-(Pc)O](BF$_4$)$_y$}$_n$ materials prepared electrochemically from tetragonal [Si(Pc)O]$_n$. Upon incremental doping, no new peaks are observed except for the reflection at $2\theta = 9°$, suggesting that the material is undergoing minimal structural changes. The reflection at $2\theta = 9°$, as expected,[7a] increases in relative intensity as y increases. This behavior is also observed with other counterions introduced by electrochemical doping, as will be discussed below. Table I sets out powder- or single-crystal-derived unit cell parameters for {[Si(Pc)O](BF$_4$)$_{0.50}$}$_n$ and related partially oxidized phthalocyanine materials. Careful analysis of the {[Si(Pc)O]-(BF$_4$)$_y$}$_n$ diffraction data as a function of y shows that, upon incremental doping, the tetragonal lattice parameters a and c change monotonically as y increases (Figure 7A). The expansion in a (+0.27 (6) Å) is expected upon anion insertion (cf. Figure 4) and the magnitude has previously been correlated with anion dimensions.[7a] The slight contraction in c (−0.03 (2) Å) (interplanar spacing × 2) is commonly observed[5b,7a] upon oxidation of such materials and presumably reflects depletion of conduction band states[6] that have ring–ring nonbonding or antibonding character. These changes in a and c are reversible within experimental error. Both of the features described above indicate the homogeneous (continuous) nature of the electrochemical doping process. Smooth variations in lattice parameters as a function of applied potential are also observed in metal chalcogenides undergoing electrochemical intercalation of Li$^+$. The bottom portion of Figure 4
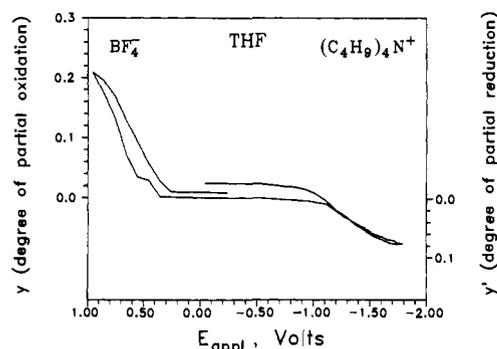
summarizes the structural aspects of [Si(Pc)O]$_n$ electrochemistry in (n-Bu$_4$N$^+$)BF$_4^-$ acetonitrile.

Transmission Infrared Spectroscopy of {[Si(Pc)O](BF$_4$)$_y$}$_n$ Materials. Figure 8 shows transmission infrared spectra of the BF$_4^-$ salts of [Si(Pc)O]$_n$ as a function of the degree of partial oxidation (y). These spectra exhibit the characteristic growth of a broad band centered around 2000 cm^{-1} due to conduction electron absorption.[5a,7a] This feature increases in prominence as y increases, indicating that the oxidized polymer is becoming more conductive. Another feature of note is that the spectra for the orthorhombic starting material and electrochemically undoped tetragonal [Si(Pc)O]$_n$ samples are identical. There is also no detectable displacement or decrease in intensity of either the phthalocyanine skeletal or Si–O chain modes upon undoping. In particular, the transition centered around 980 cm^{-1}, assigned to the locally antisymmetric Si–O–Si stretch,[5a,32a] does not shift or decrease in relative intensity, arguing that the cofacially joined polymeric structure has not been altered by the redox chemistry.

Reductive Doping Experiments. It was also of interest to determine whether [Si(Pc)O]$_n$ could be doped by electron insertion into the band constructed from metallomacrocycle lowest unoccupied molecular orbitals[6e] rather than electron extraction from the band constructed from the highest occupied molecular orbitals. Figure 9 shows a microcompaction experiment in (n-Bu$_4$N$^+$)-BF$_4^-$/THF with tetragonal [Si(Pc)O]$_n$ (see Experimental Section for details). It can be seen that the polymer can be reversibly reduced with a limiting stoichiometry for n-Bu$_4$N$^+$ insertion of $y \approx 0.09$, i.e., {(n-Bu$_4$N$^+$)$_{0.09}$[Si(Pc)O]}$_n$. It was also found that the polymer could be cycled a number of times between oxidized and reduced states with no decomposition detectable. The dif-
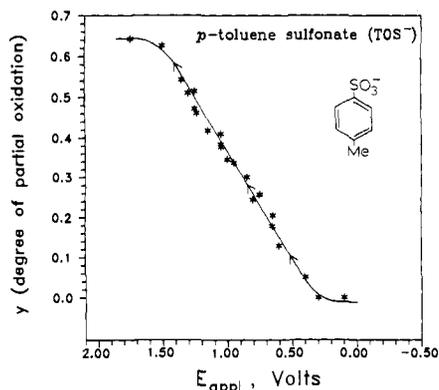
Figure 10. ECPS response of tetragonal $[Si(Pc)O]_n$ to oxidation in $(Et_4N^+)TOS^-$/acetonitrile.

Figure 12. Slurry ECPS plots for oxidation of tetragonal $[Si(Pc)O]_n$ in electrolytes composed of $(n-R_4N^+)$ salts of various counterions in acetonitrile. Legend identifies counterions.
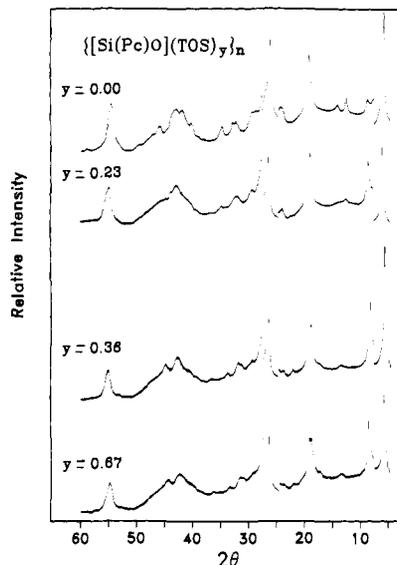
Figure 11. X-ray diffraction data for electrochemically doped polycrystalline samples of $\{[Si(Pc)O](TOS)_y\}_n$ for (A) $y = 0.00$, (B) $y = 0.23$, (C) $y = 0.36$, and (D) $y = 0.67$. Vertical scale settings in thousands of counts per second (kcps): (A, B) 5–8°, 20 kcps; 8–25°, 4 kcps; 25–28°, 20 kcps; 28–60°, 4 kcps; (C, D) 5–8°, 8 kcps; 8–25°, 4 kcps; 25–28°, 8 kcps; 28–60°, 4 kcps.

ference in potentials between oxidative and reductive doping thresholds, 1.5 V, compares favorably with the optically determined band gap of 1.65 eV (750 nm).[5a] Further studies of the extremely air-sensitive reduced polymer are in progress and will be discussed elsewhere.

Synthesis, ECPS, and X-ray Diffraction of Tosylate Salts. Slurry electrochemical oxidation of orthorhombic $[Si(Pc)O]_n$ in tetraethylammonium p-toluenesulfonate $[(Et_4N^+)TOS^-]$ as the supporting electrolyte exhibits behavior similar to that observed with BF_4^-. A similar break-in potential of 1.0–1.2 V vs SSCE and a small increase in current at early times in the electrolysis is observed. The fully doped material is formulated as $\{[Si-(Pc)O](TOS)_{0.67}\}_n$ on the basis of coulometry and elemental analysis. The X-ray powder diffraction pattern (see Supplementary Material) of $\{[Si(Pc)O](TOS)_{0.67}\}_n$ is qualitatively similar to that observed for $\{[Si(Pc)O](BF_4)_{0.50}\}_n$ (Figure 4), but the reflection intensities are considerably weaker and the lines are substantially broader, suggesting a lower degree of crystallinity. In contrast, oxidizing *tetragonal* $[Si(Pc)O]_n$ with $(Et_4N^+)TOS^-$ as the supporting electrolyte yields more crystalline doped materials, similar to those having the BF_4^- counterion (vide supra).

Figure 10 shows y vs E_{appl} data for slurry oxidation of the tetragonal $[Si(Pc)O]_n/TOS^-$/acetonitrile system. This behavior is very similar to that observed with the BF_4^- counterion. In fact, within experimental error, the degree of oxidation is the same for each anion at any potential up to 1.20 V. This result is consistent with the assertion that the material is undergoing homogeneous
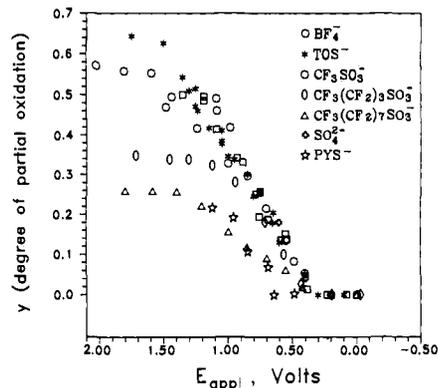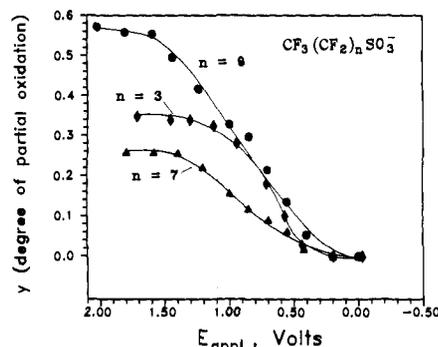
Figure 13. ECPS curves for slurry oxidation of tetragonal $[Si(Pc)O]_n$ in $(n-R_4N^+)CF_3(CF_2)_nSO_3^-$ ($n = 0, 3, 7$)/acetonitrile.

doping, that it is at the maximum degree of partial oxidation for each applied potential, and also suggests that the ECPS behavior is largely dependent on the polymer rather than the electrolyte/counterion identity. The major difference between the ECPS curves for the BF_4^- and TOS^- counterions is that the maximum degree of partial oxidation achievable for the fully doped TOS^- sample is 0.67 rather than the 0.50 observed for BF_4^-. It will be seen that the ultimate degree of oxidation achievable is markedly anion structure-sensitive.

Figure 11 presents diffraction data for $\{[Si(Pc)O](TOS)_y\}_n$ samples of varying y prepared by slurry CPC from tetragonal $[Si(Pc)O]_n$ in $(n-Bu_4N^+)TOS^-$/acetonitrile. The data are reminiscent of the $\{[Si(Pc)O](BF_4)_y\}_n$ system with the exception of a greater expansion in a [+0.70 (6) Å] and substantially broader reflections. The former no doubt reflects the greater size of TOS^-,[7a] while the latter suggests loss of crystallinity due to disorder in TOS^- packing and/or reduced coherence between parallel polysiloxane chains. The monotonic increase in a with doping (Figure 7B) is, as was the electrochemical data (Figure 10), in accord with a predominantly homogeneous doping pattern.

$[Si(Pc)O]_n$ Electrochemistry with Other Counterions. The anion dependence of the aforementioned $[Si(Pc)O]_n$ electrochemical phenomenology was investigated with R_4N^+ salts of differing anion shapes, sizes, and charges. These included tetra-n-butylammonium 1-pyrenesulfonate $[(n-Bu_4N^+)PYS^-]$, tetra-n-butylammonium hexafluorophosphate $[(n-Bu_4N^+)PF_6^-]$, tetra-n-butylammonium hexafluoroantimonate $[(n-Bu_4N^+)SbF_6^-]$, tetra-n-butylammonium trifluoromethanesulfonate $[(n-Bu_4N^+)CF_3SO_3^-]$, tetra-n-butylammonium nonafluoro-n-butanesulfonate $[(n-Bu_4N^+)NFBS^-]$, tetraethylammonium perfluoro-n-octanesulfonate $[(Et_4N^+)-PFOS^-]$, and tetra-n-butylammonium sulfate $[(n-Bu_4N^+)_2SO_4^{2-}]$. As can be seen in Figure 12, the gross electrochemical behavior of all of the salts is qualitatively similar; however, there are also interesting specific differences. First, the maximum doping level achievable is strongly dependent on the anion identity, with qualitatively "small" anions generally achieving the highest levels of insertion. It should be noted that SO_4^{2-} insertion is limited by

Table II. Maximum Degree of Partial Oxidation Observed for Electrochemically Prepared $\{[Si(Pc)O]X_y\}_n$ Materials as a Function of Counterion

counterion, X^-	maximum y^a	counterion, X^-	maximum y^a
BF_4^-	0.50	$CF_3SO_3^-$	0.55
PF_6^-	0.47	$NFBS^{-c}$	0.38
SbF_6^-	0.41	$PFOS^{-d}$	0.26
TOS^{-b}	0.67	SO_4^{2-}	0.19 (0.095)^{f,g}
PYS^-	0.22		

^{a} Measured both by coulometry and elemental analysis. ^{b} TOS^- = *p*-toluenesulfonate. ^{c} PYS^- = 1-pyrenesulfonate. ^{d} $NFBS^-$ = nona-fluoro-*n*-butanesulfonate. ^{e} $PFOS^-$ = perfluoro-*n*-octanesulfonate. ^{f} Sulfate salt is formulated as $\{[Si(Pc)O](SO_4)_{0.095}\}_n$, but $p = 0.19$. ^{g} The supporting electrolyte $(n\text{-}Bu_4N^+)_2SO_4^{2-}$ undergoes oxidation at ca. $+1.0$ V vs SSCE. The maximum y for this salt is low because E_{appl} was necessarily maintained below 0.8 V during the polymer oxidation.
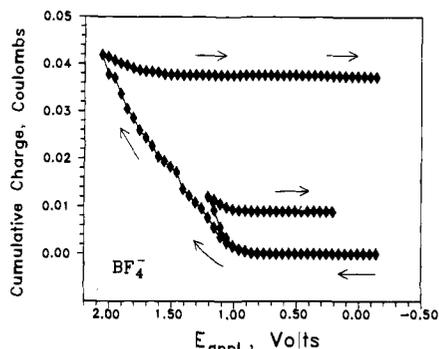
Figure 14. ECPS curves for microcompaction doping of $[Ge(Pc)O]_n$ in $(n\text{-}Bu_4N^+)BF_4^-$/acetonitrile for two different E_{appl}. The irreversibility indicates polymer decomposition.

Figure 15. (A) ECPS curves for Ni(Pc) slurry oxidation in $(n\text{-}Bu_4N^+)BF_4^-$/acetonitrile. Cycles for the β (initial) and γ (undoped) polytypes are shown. (B) ECPS data for two cycles of the microcompaction cycling of Ni(Pc) in $(n\text{-}Bu_4N^+)BF_4^-$/acetonitrile. The dashed line indicates the first cycle, the solid line the second.

the potential range within which this dianion is stable to oxidation. The homologous $CF_3(CF_2)_nSO_3^-$ series is a particularly clear-cut example of size effects (Figure 13). These size effects will be analyzed more quantitatively in the Discussion. It can also be seen from Figure 12 that for most ions, the slope of the E_{appl} vs y plot is rather similar, indicating that reorganization of the polymer lattice primarily controls the insertion process. However, deviations are noted for the largest ions, and for pyrenesulfonate, the doping threshold is displaced to higher potentials (Figure 12).[32b] Table II summarizes the maximum doping levels observed for all anions studied.

X-ray powder diffraction data were recorded for all $\{[Si(Pc)O]X_y\}_n$ materials prepared in this investigation. They are all strikingly similar to $\{[Si(Pc)O]X_y\}_n$ and $M(Pc)X_y$ data discussed and analyzed in detail elsewhere.[3,5b,7a] On this basis they have been tentatively indexed in a tetragonal crystal system. In the case of $\{[Si(Pc)O](PYS)_{0.22}\}_y$, the observed diffraction pattern is characteristic of the tetragonal $[Si(Pc)O]_n$ starting material. It is inferred from this that the salt of this very large anion is disordered/monocrystalline, hence poorly diffracting, and that the doping is inhomogeneous with the unusual ECPS response in Figure 12. Crystallographic data for $\{[Si(Pc)O]X_y\}_n$ and other partially oxidized phthalocyanine systems are summarized in Table I.

Attempted Electrochemical Doping of $[Ge(Pc)O]_n$. Electrochemical doping of $[Ge(Pc)O]_n$ was attempted in $(n\text{-}Bu_4N^+)$-BF_4^-/acetonitrile using both the microcompaction and slurry doping configurations. Figure 14 displays two ECPS curves for microcompaction attempts at two different final potentials. In both cases electrochemical oxidation is destructive to the polymer, as evidenced by the fact that attempted rereduction to neutral $[Ge(Pc)O]_n$ does not occur. Also notable was that the electrolyte solution at the completion of oxidation showed visible evidence of soluble $[Ge(Pc)O]_x$ fragments, suggesting Ge–O bond cleavage. Slurry doping experiments were also unsuccessful in that workup of the oxidized products yielded materials that did not exhibit the characteristic conduction electron absorption in the infrared[5b] (vide supra) and showed a marked diminution of the local Ge–O–Ge

stretching mode at 865 cm^{-1}.[5a,32a] These observations are similar to results obtained on attempted doping of the $[Ge(Pc)O]_n$ polymer with NO^+X^- salts.[7b]

Solid-State Electrochemistry of Ni(Pc). ECPS data for the slurry oxidation of sublimed solid Ni(Pc) in $(n\text{-}Bu_4N^+)BF_4^-$/acetonitrile are shown in Figure 15A. Data for microcompaction electrochemistry are shown in Figure 15B. Both sets of data exhibit very large overpotentials upon initial doping, indicative of a major structural reorganization and reminiscent of ortho-rhombic $[Si(Pc)O]_n$ doping. However, unlike the polymer, the undoping response of $Ni(Pc)(BF_4)_x$ ($x \approx 0.48$) is not a smooth, gently sloping function spread over a broad potential range, suggesting therefore another structural transformation. Furthermore, a second Ni(Pc) oxidation cycle is also accompanied by a steep ECPS response and an overpotential that is nearly as large as in the first cycle (Figure 15).

The seemingly complex aspects of Ni(Pc) electrochemistry are clarified by reference to the diffraction data (Figure 16). As-sublimed Ni(Pc) crystallizes in a monoclinic space group ($P2_1/a$, Figure 16A) with a herringbone, slipped-stack packing arrangement [β-Ni(Pc)].[33] The powder diffraction data are diagnostic of this phase.[34] Upon electrochemical oxidation, the diffraction data indicate a major structural transformation to the familiar stacked tetragonal ($P4/mcc$) $M(Pc)X_y$ structure (Figure 16).[3,5b,7a] This transformation explains the oxidative ECPS response. Interestingly, the limiting doping stoichiometry attained, $y \approx 0.48$, is somewhat larger than has previously been obtained by chemical oxidation[35] or galvanostatic electrocrystallization[3c] techniques. The diffraction data show that complete undoping of $Ni(Pc)(BF_4)_{0.48}$ *does not* yield an open, undoped tetragonal structure as in $[Si(Pc)O]_n$, but rather a second monoclinic ($P2_1/a$) polymorph,

(32) (a) Dirk, C. W.; Marks, T. J. *Inorg. Chem.* **1984**, *23*, 4325–4332, and references therein. (b) Preliminary doping experiments with $(n\text{-}Bu_4N^+)_4Mo_8O_{26}^{4-}$ reveal an even higher threshold (ca. $+0.9$ V vs SSCE) and a lower obtainable value of p (ca. 0.06): Schlueter, J. A.; Kellogg, G. E.; Marks, T. J., unpublished observations.

(33) Brown, C. J. *J. Chem. Soc. A* **1968**, 2494–2498.

(34) Assour, J. M. *J. Phys. Chem.* **1965**, *69*, 2295–2299.

(35) Inabe, T.; Kannewurf, C. R.; Lyding, J. W.; Moguel, M. K.; Marks, T. J. *Mol. Cryst. Liq. Cryst.* **1983**, *93*, 355–367.

Molecular Metals with Widely Tunable Band Filling

J. Am. Chem. Soc., Vol. 111, No. 14, 1989 5269
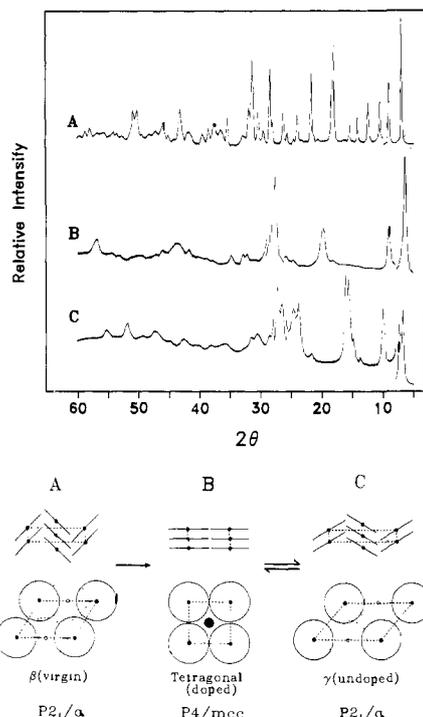
Figure 16. Top: X-ray diffraction data for polycrystalline samples of (A) β-Ni(Pc), (B) Ni(Pc)(BF$_4$)$_{0.48}$, and (C) γ-Ni(Pc) prepared by electrochemically undoping Ni(Pc)(BF$_4$)$_{0.48}$. Vertical scale settings in thousands of counts per second (kcps): (A) 5–10°, 100 kcps; 10–21°, 20 kcps; 21–40°, 10 kcps; 40–60°, 20 kcps; (B) 5–8°, 10 kcps; 8–25°, 8 kcps; 25–28°, 20 kcps; 28–60°, 8 kcps; (C) 5–8°, 20 kcps; 8–21°, 4 kcps; 21–26°, 8 kcps; 26–28°, 20 kcps; 28–40°, 8 kcps; 40–60°, 10 kcps. Bottom: crystal structure relationships in the electrochemistry of Ni-(Pc)(BF$_4$)$_y$ where y = 0.00–0.48.

normally obtained on recrystallization from acid [γ-Ni(Pc)].[34,36] This observation agrees with the aforementioned electrochemical evidence for structural rearrangement. Subsequent oxidative doping of γ-Ni(Pc) to regenerate Ni(Pc)(BF$_4$)$_{0.48}$ necessarily again involves significant structural reorganization, as underscored by the ECPS data (Figure 15).

Discussion

Polymer Structure and Electrochemistry. As evidenced by both slurry and microcompaction experiments, oxidative solid-state [Si(Pc)O]$_n$ electrochemistry is highly sensitive to crystal structure. Thus, oxidation in (n-Bu$_4$N$^+$)BF$_4^-$/acetonitrile of as-polymerized [Si(Pc)O]$_n$, which has been assigned a closely packed orthorhombic crystal structure,[5a] is accompanied by a significant overpotential and steep ECPS response. This feature can be associated with the energetic demands of *irreversibly* rearranging the [Si(Pc)O]$_n$ crystal lattice to the tetragonal architecture of the doped phase (Figures 3 and 4, "break-in"—a first-order phase transformation). In contrast, the oxidative electrochemistry of tetragonal [Si(Pc)O]$_n$, which has a more open crystal structure closely related to that of the doped phase, evidences far less, if any, overpotential, and slurry doping now allows wide, *reversible* (and preparative) tunability in y of {[Si(Pc)O](BF$_4$)$_y$}$_n$ as a function of E_{appl}—an apparently continuous structural transformation. A number of other anions can likewise be inserted in a similarly homogeneous fashion. Such behavior is, of course, limited by the intrinsic chemical stability of the [M(Pc$^{\rho+}$)O]$_n$ radical-cation assembly. In the case of [Ge(Pc)O]$_n$, oxidative doping is accompanied by competitive and irreversible cleavage of the Ge–O backbone.

The pronounced structural influence on electrochemical processes of the [Si(Pc)O]$_n$ enforced cofacial stacking architecture is clearly evident in comparative studies with Ni(Pc) in (n-

Table III. Comparison of Observed Maximum {[Si(Pc)O]X$_y$}$_n$ Doping Levels (y) and Those Estimated from Anion Packing Considerations

anion, X$^-$	van der Waals radius,[a] Å	y_{theory}[b]	y_{obsd}
BF$_4^-$	3.15	0.56	0.50
PF$_6^-$	3.35	0.52	0.47
SbF$_6^-$	3.70	0.48	0.41

[a] Calculated as sum of ionic radius of central atom, ionic radius of fluoride, and van der Waals radius of fluoride. [b] Estimated as $c/2r_{VDW}$.

Table IV. Comparison of Observed Maximum {[Si(Pc)O]X$_y$}$_n$ Doping Levels (y) and Those Estimated from Anion Packing Considerations

anion, X$^-$	van der Waals length,[a] Å	y_{theory}[b]	y_{obsd}
CF$_3$SO$_3^-$	6.4	0.52	0.55
NFBS$^-$	9.4	0.35	0.38
PFOS$^-$	15.7	0.21	0.26

[a] Calculated from ionic and van der Waals radii of component elements. Valence angles (sp^3) of 109° are assumed. [b] Estimated as c/l_{VDW}.

Bu$_4$N$^+$)BF$_4^-$/acetonitrile. As-sublimed Ni(Pc) crystallizes in a monoclinic ($P2_1/a$, β-polytype) herringbone packing arrangement (Figure 16). Electrochemical oxidation proceeds with a large overpotential (greater than in orthorhombic [Si(Pc)O$_n$]) and over a rather narrow potential range. This major structural reorganization yields the tetragonal doped phase. However, unlike the cofacially joined polymer system, undoping also occurs with a significant overpotential, there is little tunability in band filling,[37] and in the absence of a structure-enforcing (–SiO–)$_n$ backbone, the M(Pc) packing collapses to a slipped-stack monoclinic structure [γ-Ni(Pc)]. The formation of the γ- rather than β-Ni(Pc) polytype in this process apparently reflects the greater similarity in lattice parameters (and Ni(Pc) tilt angle) to the tetragonal doped crystal structure. Thus, every cycle in Ni(Pc) redox chemistry is accompanied by a major structural rearrangement and attendant electrochemical hysteresis. Such behavior would clearly have significant, deleterious consequences for applications such as energy storage devices.

Anion Effects on Electrochemistry. In earlier studies of [Si(Pc)O]$_n$ doping using chemical oxidants, it was argued from thermodynamic considerations that maximum doping stoichiometry levels achieved were largely a function of the oxidizing characteristics of the dopant.[7a] Electrochemical approaches considerably relax such contraints, and in the present work, wide variations in doping stoichiometry/band filling are observed with limiting levels clearly discernible from ECPS data. With the exception of obvious constraints imposed by anion and polymer redox stabilities, it will be seen for a broad range of anion types that the ultimate doping stoichiometry/band filling levels (y) that can be achieved for {[Si(Pc)O]X$_y$}$_n$ materials are primarily structural in origin.

As discussed above, the crystal structures of M(Pc)X$_y$ and {[M(Pc)O]X$_y$}$_n$ materials consist of M(Pc) stacks and parallel arrays of off-axis counterions located in "tunnels" defined by surrounding walls of lipophilic benzo C–H groups (Figure 4). The approximate van der Waals radius of this tunnel must be sufficiently large to accommodate the X$^-$ anions, and in the NO$^+$X$^-$-doped {[Si(Pc)O]X$_y$}$_n$ series, the a axis length could be approximately correlated with X$^-$ dimensions (BF$_4^-$, PF$_6^-$, SbF$_6^-$).[7a] Here y was limited by the oxidizing power of NO$^+$. To determine whether electrochemical y values reflect structural constraints, calculations were made of the maximum number of anions that can be packed in a chain along c in the {[Si(Pc)O]X$_y$}$_n$ crystal structure. Trial calculations with BF$_4^-$, PF$_6^-$, and SbF$_6^-$ employed spherical anion van der Waals radii estimated from component atom ionic radii[38] and the fluorine van der Waals radius.[39] As

(36) Brown, C. J. *J. Chem. Soc. A* **1968**, 2488–2493.

(37) The ECPS data do imply some stoichiometric tunability in Ni-(Pc)(BF$_4$)$_{0.48}$ undoping. Evidence for this is also found in the variable stoichiometries observed in the Ni(Pc)(ClO$_4$)$_y$ series.[3a]

(38) Shannon, R. D. *Acta Crystallogr.* **1976**, *A32*, 751–767.

5270 *J. Am. Chem. Soc., Vol. 111, No. 14, 1989*

Gaudiello et al.

can be seen in Table III, the agreement between observed and calculated stoichiometries based entirely upon packing considerations is good. For perfluoroalkylsulfonate anions, similar calculations were carried out using published metrical parameters for fluorocarbon and perfluoroalkylsulfonate molecules[40] as well as appropriate van der Waals radii.[39] Long-chain perfluoroalkyl groups were assumed to be linear and planar.[40d,e] As can be judged from Table IV, there is again good agreement between maximum stoichiometries calculated on the basis of van der Waals lengths and those observed experimentally.[41]

Trial packing calculations were also carried out for tosylate packing in {[Si(Pc)O](TOS)$_y$}$_n$ using published metrical[42] and van der Waals radius[39] parameters. The crystallographic data (Table I) indicate that the anion tunnel diameter is ca. 0.1–0.2 Å larger than for SbF$_6^-$, i.e., ca. 7.5 Å. These calculations and experiments with space-filling models indicated that stoichiometries in the y $\approx$ 0.6 range could be achieved in several packing motifs. Slipped-stack patterns came closest to $y \approx 0.67$ with only minor compression of van der Waals distances.

Comparison to Other Molecular and Polymeric Metals. In general, molecular metals crystallize in fixed oxidation states (band fillings) for a given crystal structure.[1] Major excursions in oxidation states are usually attended by very large changes in crystal structure, as exemplified by the TTF halides.[2b,43] Those factors governing crystallization and band-filling patterns in molecular metals reflect a complex interplay of difficulty quantified Madelung, exchange, polarization, covalent, and van der Waals forces.[7a,44,45] However, it is now clear that overall lattice energies in most of these materials are rather small (ca. 3–10 kcal/mol)[7a,46] so that variations in crystal structure and oxidation state as well as simultaneous crystallization of several phases should not be surprising. Cases where nonnegligible variation in oxidation state occurs for a given crystallization architecture largely fall into two categories. In the first (A), columnar D$_n$ donor stacks incorporate
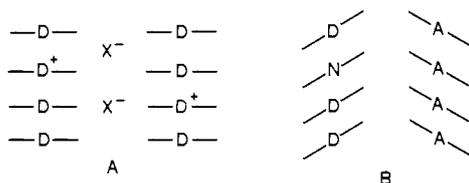
varying quantities of counterions in parallel, off-axis tunnels. In most cases, the counterions are considerably smaller and cylindrical or spherical in shape. Examples of this motif include TTF^{y+}X$_y^-$ where X$^-$ = halide and $y \approx 0.8$[43b] or M(Pc$_y^+$)X$_y^-$ where X = e.g., ClO$_4^-$ and $y \approx 0.40$.[3a] The other type of system with variable band filling is exemplified by (NMP)$_x$(Phen)$_{1-x}$(TCNQ) in which neutral molecules (N, phenazine) are alloyed in a molecular donor

(D, *N*-methylphenazine)/acceptor (A, TCNQ) lattice (B).[9] In both types of materials, the tunability in band filling is significantly less than 0.2 electrons/site, and all evidence is that further excursions cannot be effected without major changes in the crystal structure. For example, in Ni(Pc)(BF$_4$)$_y$ (vide supra), collapse of the crystal structure from D$_n$ to slipped stacking occurs when y falls below a certain level. The tunability of band filling in the present cofacially joined phthalocyanine polymers is clearly a radical departure in behavior.

In addition to the present {[Si(Pc)O]X$_y$}$_n$ conductive polymers, electrochemical/structural relationships have been extensively investigated for *trans*-polyacetylene. Considerably more information is presently available for reductive doping[25d,47] (alkali-metal insertion) than for oxidative doping.[47a,48,49] In both cases, however, the picture is rather different than for {[Si(Pc)O]X$_y$}$_n$ oxidative doping. Initial doping of polyacetylene is invariably found to be inhomogeneous, with the coexistence of undoped (or lightly doped) and doped [(CHX$_y$)$_n$, $y \approx 0.06$] phases. Then, depending on the counterion, transformations are observed upon further doping to different polymer chain/counterion packing arrangements and/or there is a modest tunability in band filling for a given crystal structure. However, in no case is the overall limiting degree of charge storage per polymer subunit as great as in the phthalocyanine polymer nor is there comparable tunability in band filling. These differences no doubt reflect the far larger dimensions of the delocalized phthalocyanine π systems and the attendant demonstrated capacity to store positive or negative charge[49] as well as the far closer polyacetylene–counterion interactions. The latter is understandable vis-à-vis {[Si(Pc)O]X$_y$}$_n$ systems in terms of the higher concentration of charge per polyacetylene subunit and a polymer structure that is favorable for close π-system–counterion interactions (especially for alkali metal[47] or polyhalide ions[48d,e]). The magnitudes of these interactions no doubt favor different polyacetylene packing arrangements for different stoichiometries or counterions, while we have previously shown that direct π-system–counterion interactions are small for structure-enforced phthalocyanine conductors.[7a] The factors mentioned above also suggest that doped polyacetylene crystal structures will collapse upon undoping and that well-ordered "broken-in" crystal structures, which are more amenable to facile doping/undoping cycles, will not be accessible. Existing polyacetylene data appear to confirm this.[11,48,50]

Conclusions

From the standpoint of electrically conductive polymers, the present study illustrates the great sensitivity of electrochemical phenomena to polymer chain architecture (subunit packing, connectivity, geometry, electronic structure) and counterion structure. From the standpoint of molecular metals, the {[Si(Pc)O]X$_y$}$_n$ systems represent the only system to date where wide tunability in band filling and counterion identity is possible. How the electrical, optical, and magnetic properties of such a molecular metal respond to such tuning is the subject of the accompanying contribution.[12]

(39) Huheey, J. E. *Inorg. Chemistry*, 3rd ed.; Harper and Row: New York, 1983; pp 258–259.

(40) (a) Gallaher, K. L.; Yokozeki, A.; Bauer, S. H. *J. Phys. Chem.* **1974**, *78*, 2389–2395. (b) Gänswein, B.; Brauer, G. *Z. Anorg. Allg. Chem.* **1975**, *415*, 125–132. (c) Hjortaas, K. E.; Strømme, K. O. *Acta Chem. Scand.* **1968**, *22*, 2965–2971. (d) Clark, E. S.; Muus, L. T. *Z. Kristallogr.* **1962**, *117*, 119–127. (e) Bastiansen, O.; Hadler, E. *Acta Chem. Scand.* **1952**, *6*, 214–218.

(41) The slightly larger underestimate of y in the case of CF$_3$(CF$_2$)$_7$SO$_3^-$ and the slightly larger a parameter in the corresponding crystallographic data (Table I) may indicate some helicity[40d] in the CF$_3$(CF$_2$)$_7$-chain structure.

(42) Lundgren, J.-O.; Williams, J. M. *J. Chem. Phys.* **1973**, *58*, 788–796.

(43) (a) Teitelbaum, R. C.; Marks, T. J.; Johnson, C. K. *J. Am. Chem. Soc.* **1980**, *102*, 2986–2989, and references therein. (b) Scott, B. A.; La Placa, S. J.; Torrance, J. B.; Silverman, B. D.; Welber, B. *J. Am. Chem. Soc.* **1977**, *99*, 6631–6639.

(44) Marks, T. J.; Dirk, C. W.; Schoch, K. F., Jr.; Lyding, J. W. In *Molecular Electronic Devices*; Carter, F. L., Ed.; Marcel Dekker, Inc.: New York, 1982; pp 195–210.

(45) (a) Wiygul, F. M.; Metzger, R. M.; Kistenmacher, T. J. *Mol. Cryst. Liq. Cryst.* **1984**, *107*, 115–131. (b) Metzger, R. M. *J. Chem. Phys.* **1981**, *75*, 3087–3096. (c) Torrance, J. B.; Silverman, B. D. *Phys. Rev. B* **1977**, *15*, 788–801. (d) Epstein, A. J.; Lipari, N. O.; Sandman, D. J.; Nielsen, P. *Phys. Rev. B*, **1976**, *13*, 1569–1579.

(46) (a) Pietro, W. J.; Marks, T. J., submitted for publication. (b) Metzger, R. M. *J. Chem. Phys.* **1977**, *66*, 2525–2533. (c) Metzger, R. M.; Arafat, E. S. *J. Chem. Phys.* **1983**, *78*, 2696–2705. (d) Metzger, R. M.; Arafat, E. S.; Kuo, C. S. *J. Chem. Phys.* **1983**, *78*, 2706–2709.

(47) (a) Chen, J.; Heeger, A. G. *Synth. Met.* **1988**, *24*, 311–327. (b) Winokur, M.; Moon, Y. B. Heeger, A. J.; Barker, J.; Bott, D. C.; Shirakawa, H. *Phys. Rev. Lett.* **1987**, *58*, 2329–2932. (c) Moon, Y. B.; Winokur, M.; Heeger, A. J.; Barker, J.; Bott, D. C. *Macromolecules* **1987**, *20*, 2457–2461. (d) Bott, D. C.; Brown, C. S.; Winter, J. N.; Barker, J. *Polymer* **1987**, *28*, 601–616.

(48) (a) Wieners, G.; Weizenhöfer, R.; Monkenbusch, M.; Stamm, M.; Lieser, G.; Enkelmann, V.; Wegner, G. *Makromol. Chem., Rapid Commun.* **1985**, *6*, 425–431. (b) Pouget, J. P.; Pouxviel, J. C.; Robin, P.; Comes, R.; Begin, D.; Billaud, D.; Feldblum, A.; Gibson, H. W.; Epstein, A. J. *Mol. Cryst. Liq. Cryst.* **1985**, *117*, 75–82. (c) Hässlin, H. W.; Riekel, C.; Menke, K.; Roth, S. *Makromol. Chem.* **1984**, *185*, 397–416. (d) Baughman, R. H.; Murthy, N. S.; Miller, G. G. *J. Chem. Phys.* **1983**, *79*, 515–520. (e) Chien, J. C. W.; Karasz, F. E.; Shimamura, K. *Macromolecules* **1982**, *15*, 1012–1017.

(49) (a) Wheeler, B. L.; Nagasubramanian, G.; Bard, A. J.; Schechtman, L. A.; Dininny, D. R.; Kenney, M. E. *J. Am. Chem. Soc.* **1984**, *106*, 7404–7410. (b) Mezza, T. M.; Armstrong, N. R.; Ritter, G. W., II; Iafalice, J. P.; Kenney, M. E. *J. Electroanal. Chem.* **1982**, *137*, 227–237.

(50) Maxfield, M.; Jow, T. R.; Gould, S.; Sewchok, M. G.; Shacklette, L. W. *J. Electrochem. Soc.* **1988**, *135*, 299–305.

Molecular Metals with Widely Tunable Band Filling. Response of the Collective Properties of a Phthalocyanine Molecular Metal to Drastic Excursions in Partial Oxidation State and Charge-Compensating Counterions

Manuel Almeida,[1a] John G. Gaudiello,[1a] Glen E. Kellogg,[1a] Stephen M. Tetrick,[1a] Henry O. Marcy,[1b] William J. McCarthy,[1b] John C. Butler,[1b] Carl R. Kannewurf,[1b] and Tobin J. Marks*,[1a]

Contribution from the Department of Chemistry, the Department of Electrical Engineering and Computer Science, and the Materials Research Center, Northwestern University. Evanston, Illinois 60208. Received July 18, 1988

Abstract: The electrical, optical, and magnetic properties of the partially oxidized, cofacially joined phthalocyanine polymers {[Si(Pc)O]X$_y$}$_n$ are investigated for X⁻ = BF₄⁻, y = 0.00–0.50; X⁻ = p-toluenesulfonate (TOS⁻), y = 0.00–0.67; and X⁻ = SO₄²⁻. y = 0.040, 0.095. As a function of increasing y, the physical properties of the BF₄⁻ and TOS⁻ salts evidence a transition at $y \approx 0.20$ from a localized carrier semiconductor or insulator to a molecular metal. Thus, the dc electrical conductivity increases from low values having a temperature dependence most characteristic of disorder and/or hopping transport between localized states to values characteristic of a molecular metal with fluctuation-induced carrier tunneling between relatively large metallike particles. Beyond $y \gtrsim 0.25$, the conductivity is only weakly dependent on y. At $y \approx 0.20$, the thermoelectric power [$S(T)$] also changes from behavior characteristic of a p-type semiconductor or insulator to that of a p-type molecular metal. Differences in $S(T)$ between X⁻ = BF₄⁻ and TOS⁻ polymers appear to be due largely to minor structural variations. Optical reflectivity measurements reveal the appearance of a metallike plasma edge at $y \approx 0.20$, followed by an incremental shift of this feature to higher energy with further increase in y. The static magnetic susceptibility of {[Si(Pc)O](BF₄)$_y$}$_n$ evidences an abrupt transition at $y \approx 0.20$ from a large concentration of localized, Curie-like spins to Pauli-like behavior characteristic of a molecular metal. Beyond $y \gtrsim 0.30$, the Pauli-like susceptibility is nearly independent of y. ESR studies indicate a ligand-centered π-radical-cation electronic structure. For X⁻ = BF₄⁻ and TOS⁻, line-width studies as a function of y evidence a progression from relatively localized to delocalized carriers. It is suggested that the insulator/semiconductor to molecular metal transition in these materials is an Anderson-like transition that arises when the Fermi level crosses a mobility edge from localized states (presumably due to disorder and/or defects) at the tail of the conduction band to delocalized, metallike states. With the possible exception of ESR line-width data, the electrical, optical, and magnetic studies of {[Si(Pc)O](SO₄)₀.₀₉₅}$_n$ provide no evidence for an enhanced, carrier-localizing perturbation of the [Si(Pc$^{\rho+}$)O]$_n$ band structure by the dinegative off-axis counterions.

In the preceding contribution,[2] we discussed chemical, structural, and thermodynamic aspects of electrochemically oxidizing ("doping") the cofacially joined metallophthalocyanine polymer [Si(Pc)O]$_n$ to yield products of the type {[Si(Pc)O]X$_y$}$_n$. Under conditions in which molecular stacking is rigorously enforced, it was shown to be possible not only to effect significant variation in X⁻, but also to achieve wide and continuous tuning of the conduction band filling, $(2 - y)/2$. Such counterion and band-filling tunability with invariant stacking has not previously been achievable to any major extent for any conventional molecular conductor.[3] Since partially oxidized stacked molecular metal-

lophthalocyanines form the basis for a broad class of predominantly ligand-centered molecular metals,[4,5] it was of great interest to learn how the collective properties of a stacking-enforced, metallike phthalocyanine assembly would respond to the tuning of such perturbations.

We report here a combined charge-transport (variable-temperature conductivity and thermoelectric power), optical spectroscopic, and magnetic investigation of the {[Si(Pc)O]X$_y$}$_n$ system for both a small, nonpolarizable counterion (X⁻ = BF₄⁻, y = 0–0.50), and a large, polarizable, aromatic counterion (X⁻ =

(1) (a) Department of Chemistry and the Materials Research Center. (b) Department of Electrical Engineering and Computer Science and the Materials Research Center.

(2) Gaudiello, J. G.; Kellogg, G. E.; Tetrick, S. M.; Marks, T. J. *J. Am. Chem. Soc.*, preceding paper in this issue.

(3) (a) *Proc. Int. Conf. Sci. Technol. Synth. Met. Synth. Met.* **1987**, *17–19*. (b) Jérome, D., Caron, L. G., Eds. *Low-Dimensional Conductors and Superconductors*; Plenum: New York, 1987. (c) Ferraro, J. R.; Williams, J. M. *Introduction to Synthetic Electrical Conductors*; Academic Press: New York, 1987. (d) Becker, J. Y., Bernstein, J., Bittner, S., Eds. *Isr. J. Chem.* **1986**, *27*(4). (e) Cowan, D. O.; Wiygul, F. M. *Chem. Eng. News* **1986**, *64*, 28–45. (f) Cohen, M. L. *Science* **1986**, *234*, 549–553. (g) Williams, J. M. *Prog. Inorg. Chem.* **1985**, *33*, 183–220. (h) Wudl, F. *Acc. Chem. Res.* **1984**, *17*, 227–232. (i) Greene, R. L.; Street, G. B. *Science* **1984**, *226*, 651–656. (j) Miller, J. S., Ed. *Extended Linear Chain Compounds*; Plenum: New York, 1982; Vol. 1–3.

(4) Marks, T. J. *Science* **1985**, *227*, 881–889.

(5) (a) Almeida, M.; Kanatzidis, M. G.; Tonge, L. M.; Marks, T. J.; Marcy, H. O.; McCarthy, W. J.; Kannewurf, C. R. *Solid State Commun.* **1987**, *63*, 457–461. (b) Inabe, T.; Liang, W.-B.; Lomax, J. F.; Nakamura, S.; Lyding, J. W.; McCarthy, W. J.; Carr, S. H.; Kannewurf, C. R.; Marks, T. J. *Synth. Met.* **1986**, *13*, 219–229. (c) Gaudiello, J. G.; Marcy, H. O.; McCarthy, W. J.; Moguel, M. K.; Kannewurf, C. R.; Marks, T. J. *Synth. Met.* **1986**, *15*, 115–128. (d) Inabe, T.; Nakamura, S.; Liang, W.-B.; Marks, T. J.; Burton, R. L.; Kannewurf, C. R.; Imaeda, K.-I. *J. Am. Chem. Soc.* **1985**, *107*, 7224–7226. (e) Inabe, T.; Marks, T. J.; Burton, R. L.; Lyding, J. W.; McCarthy, W. J.; Kannewurf, C. R.; Reisner, G. M.; Herbstein, F. H. *Solid State Commun.* **1985**, *54*, 501–504. (f) Martinsen, J.; Palmer, S. M.; Tanaka, J.; Greene, R. C.; Hoffman, B. M. *Phys. Rev. B* **1984**, *30*, 6269–6276. (g) Yakushi, K.; Sakuda, M.; Hamada, I.; Kuroda, H.; Kawamoto, A.; Tanaka, J.; Sugano, T.; Kinoshita, M. In ref 3a, *19*, 769–774. (h) Schramm, C. J.; Scaringe, R. P.; Stojakovic, D. R.; Hoffman, B. M.; Ibers, J. A.; Marks, T. J. *J. Am. Chem. Soc.* **1980**, *102*, 6702–6713.